8-1-2019

High-Precision Radioisotopic Ages for the Lower Midian (Upper Wordian) Stage of the Tethyan Time Scale, Shigeyasu Quarry, Yamaguchi Prefecture, Japan

V. I. Davydov
Boise State University

M. D. Schmitz
Boise State University

Publication Information

Davydov, V.I. and Schmitz, M.D. (2019). "High-Precision Radioisotopic Ages for the Lower Midian (Upper Wordian) Stage of the Tethyan Time Scale, Shigeyasu Quarry, Yamaguchi Prefecture, Japan". *Palaeogeography, Palaeoclimatology, Palaeoecology, 527*, 133-145. doi: https://doi.org/10.1016/j.palaeo.2019.04.008

High-precision radioisotopic ages for the lower Midian (upper Wordian) Stage of the Tethyan ~~Time~~ time ~~Scale~~scale, Shigeyasu Quarry, Yamaguchi Prefecture, Japan.

Davydov, V. I.[1,2,3], and Schmitz, M. D.[1]

[1]Department of Geosciences, Boise State University, Boise, ID, 83725, USA (vdavydov@boisesate.edu)

[2] Kazan Federal University, 18 Kremlyovskaya St., Kazan, Republic of Tatarstan 420008, Russia

[3] North-East Interdisciplinary Scientific Research Institute n. a. N.A. Shilo Far East Branch of the Russian Academy of Sciences, Magadan

* Corresponding author: vdavydov@boisestate.edu

Abstract.

Global correlation of strata to the Guadalupian Series ~~Epoch~~ (Permian Period) of the International Geologic Time Scale remains provisional due to a lack of ~~many~~ the sufficient biostratigraphically constrained radioisotopic ages. Five new ~~CA-IDTIMS~~high-precision U-Pb radioisotopic ages were obtained from tuffs in the lower Midian (upper Wordian) volcano-siliciclastic succession of the Akiyoshi Plateau, southwestern ~~-~~Japan. Two undisturbed and continuous tuffs occur within fusulinid-bearing laminated limestone turbidites, ~~that provide~~ with precise biostratigraphic control. The *Colania douvillei* and *Lepidolina shiraiwensis* fusulinid Zones in the Akiyoshi succession provide an early Midian age in the Tethyan provincial ~~Permian Timescale~~ time scale. The range of ages (267.46 ± 0.04 Ma to 265.76 ± 0.03 Ma) over 25 m of section including the limestone turbiditic beds suggest that this ~~early~~ lower Midian ~~sequence~~ Stage of the Tethyan time scale ~~Scale~~ is ~~thus~~ correlated with the upper Wordian Stage of the International Geologic Time Scale. The sedimentologic, bio- and geochronologic data affirm the effectively conformable nature of the siliciclastic-carbonate succession of the Tsunemori

Formation at the Shigeyasu Quarry, and the presence of acidic volcanic tuffs are consistent with a forearc basin or trench slope basin depocenter for the Tsunemori Formation.

~~The sedimentologic, bio- and geochronologic data that are proving a normal sedimentary succession~~~~The obtained radioisotopic, sedimentologic and biostratigraphic data of the Tsunemori Formation at the Shigeyasu Quarry and the presence of acidic volcanic tuffs are consistent with the newly proposed model of the forearc basin or trench slope basin as sedimentation site for the entire Tsunemori Formation.~~

~~1.~~ **Key words:** Guadalupian (middle Permian); Tethyan Timescale; CA-IDITIMS, fusulinids biostratigraphy; correlation.

~~2.~~1. Introduction~~.~~

Significant progress has been made in the last decade on the radioisotopic calibration of the International Geologic Time Scale (IGTS)~~,~~ (Gradstein et al., 2012; Cohen et al., 2013) ~~but~~ yet some parts of the scale are still calibrated only provisionally. This is particularly true for the ~~upper~~ late Cisuralian (post ~~early~~ Artinskian) and Guadalupian ~~Series~~ Epoch of the Permian ~~9280~~(280-265 Ma), where just a few reliable high precision U-Pb ages exist (Henderson et al., 2012). This part of the Permian Time Scale that is calibrated~~-~~ only with biostratigraphic scaling requires further geochronologic improvement~~This part of the Permian Time Scale is thus calibrated with biostratigraphic scaling and requires further improvement~~. The paleobiogeographic provinciality and the lack of the radioisotopic calibration of this part of the scale make the correlation of Guadalupian Series and Stages in the type region with the rest of the world difficult. ~~Besides the lack of the radioisotopic calibration, there is an issue of the paleobiogeographic provinciality, and correlation of the Stages~~ stages ~~of the Guadalupian Epoch~~

~~Series in the type region with the marine Tethyan Scale time scale, as well as continental successions all over the world.~~ The only ~~TIMS~~ calibrating radioisotopic age in the entire Guadalupian in the type area ~~came~~ is from a volcanic ash ~~occurred~~ between the Hegler and Pinery limestone members of the Bell Canyon Formation at Nipple Hill, Guadalupe Mountains National Park, Texas. The ash is 6 to 8 cm thick and lies 2 m above the top of the Hegler Member, within the undifferentiated Bell Canyon Formation, and 20 m below the base of the *Jinogondolella postserrata* conodont ~~zone~~ Zone and the base of the Capitanian Stage (Bowring et al., 1998). The original legacy age of 265.3 ± 0.2 Ma for this volcanic tuff was recently revised using the chemical abrasion isotope dilution thermal ionization mass spectrometry (CA-IDTIMS) method (Mattinson, 2005) to 265.46 ± 0.27 Ma (Ramezani and Bowring, 2018).

Several CA-IDTIMS radioisotopic ages were recently published from the base of Kuhfengian in South China (Wu et al., 2017) and from the analogues of the Roadian (Russian-Omolonian and Olynian Regional Stages in N-E of Russian) and Capitanian (Gizhigian Regional Stage) in N-E of Russia (Davydov et al., 2016; Davydov et al., 2018). The latter publication suggests a new calibration of the entire Guadalupian Epoch and proposes the extension of the base of the Roadian down to 277 Ma and the Wordian down to 271 Ma. The EARTHTIME isotope dilution tracer ~~has been~~was utilized in all of these studies, ~~that aids~~which aids ~~directly compare~~in the direct comparison of the dates from Texas, Russia and South China.

~~Nevertheless, the~~ The correlation between the type section of the Guadalupian Series in Texas and the Tethyan ~~Scale~~ time scale remains quite controversial (Davydov et al., 2018). Specifically, we do not know the exact analogues of all three stages of the Guadalupian Series in the Tethyan time Scale. The report in this study of new ~~CA-IDTI~~ high-precision MS radioisotopic U-Pb zircon ages ~~reported in this study from~~for the lower Midian Stage of Japan is one ~~more~~ step towards that correlation ~~of the Tethyan to the International Geologic Time~~. The fusulinid fauna within the limestone turbidites and limestone slump blocks intercalated with the dated volcanic ashes are consistently early Midian in age and therefore can refine the maximum age of ~~the~~ that ~~Stage~~ stage in the Tethyan ~~Geologic Time Scale (TTS~~ time scale) and ~~consequently~~ its correlation to an ~~late~~ upper Wordian Stage in the ~~International Geologic Time Scale (~~IGTS~~)~~.

~~3.~~2. Geological ~~Setting~~ setting~~.~~

~~The~~ Samples for the present study were collected ~~in~~ at Shigeyasu Quarry, in rocks of the Akiyoshi Belt, ~~that~~ which is distributed ~~in~~ across several isolated areas of the Inner Zone of Southwestern Japan, extending into the western margin of the Hida Belt (Wakita, 2013). The Akiyoshi Belt forms a Permian accretionary complex (Fig. 1) composed of sandstone, mudstone, conglomerate, siliceous shale, felsic tuff, chert, limestone and basalt. The Permian Akiyoshi accretionary complex is divided into two units, which show similar ages but distinctly different dominant lithologies: a limestone-rich unit consisting of several large limestone plateaus that belong~~s~~ to the Akiyoshi Limestone Group ~~Limestone. The~~, and a second unit that is composed mainly of siliciclastic successions with minor volcanic components, named ~~as~~ the Tsunemori Formation. Both units formed by continuous sedimentation through the same period (Sano and Kanmera, 1991a; Tazawa et al., 2009). Many components of this belt are unmetamorphosed and the limestone within the belt is famous for its well preserved and diverse fauna (Toriyama, 1967). The Tsunemori Formation is unconformably overlain by Triassic shallow marine to non-marine sedimentary rocks of the Mine Group.

The Akiyoshi Limestone Group covers almost the whole area of the Akiyoshi Plateau in the central part of Yamaguchi Prefecture, southwest Japan. The Akiyoshi Limestone Group is a reefal limestone on a seamount in the Panthalassan Ocean (Kanmera and Nishi, 1983), and is one of the most complete and continuous carbonate successions in the Panthalassa region, ranging from Early Carboniferous to Middle Permian in age (Toriyama, 1967).

The Tsunemori Formation along the marginal parts of the western Akiyoshi-dai ~~plateau~~Plateau, southwest Japan, ~~are~~ is described as a sequence of broken limestone, limestone breccia, and scaly mudstone (Sano and Kanmera, 1991b), designated as evidence of melange formation caused during subduction and accretion. The broken limestone is characterized by penetrative and pervasive destruction of skeletal grains and primary sedimentary fabrics. The ~~Kasimovian, Gzhelian, Asselian, Sakmarian, and Artinskian~~ Late Visean to Midian foraminifera from the same depositional period as the entire Akiyoshi Limestone Group are identified in the broken limestone, but with no orderly stratigraphic succession (Sano and Kanmera, 1991a; Tazawa et al., 2009; Kobayashi, 2012c). The Tsunemori Formation according ~~these~~ the first authors is a trench deposit, with the Akiyoshi Limestone accreted as an exotic block sometime~~s~~ during Middle to Late Permian time, based upon radiolarian biostratigraphy (Sano and Kanmera, 1991c).

An alternative ~~new~~ model ~~of~~ for ~~the~~ Tsunemori Formation sedimentation ~~processes~~ and depositional setting has been proposed recently in the territory west ~~from~~ of the Akiyoshi-dai

~~plateau~~Plateau, that includes the area of our study (Wakita et al., 2018). ~~The normal stratigraphic stratified~~ A comfortable succession of mudstone and mudstone~~-~~-dominant turbidite with very thin layers of sandstone or siltstone and rare horizons of calcarenite and limestone breccia is documented there. No fissility or ~~and~~ scaly cleavage ~~are~~ is recognized in the mudstone and pebbly mudstone of the Tsunemori Formation (Wakita et al., 2018). The ~~deformation style of the rocks of the Tsunemori Formation are different from~~lack of penetrative deformations is inconsistent with sedimentary formations deposited at the trench and ~~accreted to form an accretionary wedge, and~~ rather ~~best fit with~~ suggests a forearc basin or trench slope basin as the sedimentation site for the Tsunemori Formation (Wakita et al., 2018). Our brief field investigation of the Tsunemori Formation at Shigeyasu Quarry ~~also suggests~~ documents that the formation ~~generally stratified, although in places the rock~~ is faulted and ~~bended folded~~ overturned, but generally stratified (Fig. 2). We found three types of ~~sedimentation of the~~ limestone within the Tsunemori Formation: 1) rare horizons of clastic limestone ~~within~~ interbedded with ~~the~~ debris flows and turbidites; 2) fully isolated blocks (2x3 m) of limestone (10VD98), wholly embedded in mudstone, i.e. slump block; 3) laminated limestone turbidite (10VD21, 22,23) ~~that is laterally pinched out~~ (Figs. 2-3). ~~All f~~Fusulinid samples ~~we collected~~ from all ~~these~~ three types of the limestone possessed the same early Midian age fauna.

Acidic volcanism in the late Guadalupian and Lopingian of Japan in general, and specifically volcanic rocks in the ~~Capitanian~~ upper Guadalupian of the Akyioshi Group have long been recognized (Kanmera, 1974). Recent provenance and petrologic studies confirm the presence of a volcanic arc system near by the Akiyoshi terrane during entire Permian time (Okawa et al., 2013; Hara et al., 2018; Zhang et al., 2018).

~~4.~~3. Materials and ~~Methods~~methods

Five samples of volcanic ~~ash beds~~ tuffs and four samples ~~from~~ of limestone ~~turbidites~~ were collected in the succession of the lower Tsunemori Formation exposed along the north-east to south-west edge of Shigeyasu Quarry (Fig. 2). The samples for ~~the~~ radioisotopic ~~studies~~ study were collected from ~~completely altered to bentonite~~bentonitic volcanic tuff layers that ~~frequently~~ occur within the lower part of the succession (Fig. 3). Three horizons were sampled from within siliciclastic beds 1.7, 5, and 20 meters below the base of a prominent bar of laminated limestone turbidite beds (samples 10VD26, 10VD95, and 10VD96, respectively). Two tuff samples were collected ~~from~~ within the laminated limestone turbiditic beds~~es~~ near their base and top (samples 10VD25 and 10VD20 respectively), thus bracketing several of the fusulinids samples (Figs. 2-3). All tuffs are laterally traceable within the exposure of the Tsunemori Formation at the quarry.

All tuffs were processed with standard procedures including ultrasonic disaggregation and concentration (Hoke et al., 2014), Franz magnetic separation, heavy liquid separation, and hand picking. All samples yielded hundreds of sharply facetted, prismatic zircon grains (Figs. 2-3). The procedure and approaches associated with chemical-abrasion isotope dilution thermal ionization mass-spectrometry (CA-IDTIMS) method have been recently described in detail by Davydov et al. (2018). CA-IDTIMS dates are reported with weighted mean uncertainties given as ± X/Y/Z, where X is the 2σ analytical uncertainty, Y is the combined analytical and tracer uncertainty (value given in parentheses), and Z is the combined analytical, tracer, and decay constant uncertainty [value given in brackets]. ~~All samples yield great amount several hundreds of excellent prismatic zircon grains (Figs.2-3).~~ The limestone samples were sliced into plates and fifty-one thin-sections with oriented fusulinids sections were prepared.

~~The field inclination of the rock suggests the younger rocks of Tsunbemori Formation occur in the north-eastern corner of the edge of the quarry (Fig. 2). However, it turns that CA-IDTIMS radioisotopic ages a suggest the overturned position orientation of the succession (Figs. 3-4), that which is a common feature within the Tsunemori Formation~~ (Wakita et al., 2018)~~.~~

~~5.~~4. Biostratigraphic results

We acknowledge that fusuilinid-bearing limestone turbidites (debris flows) are allochthonous with respect to the deeper water syn-sedimentary siliciclastic rocks, ~~the~~ and thus their biostratigraphic constraints would generally only constrain the maximum depositional age of such a stratigraphic succession. In this case, however, ~~the presence of~~ volcanic ash beds at the base and within the laminated turbiditic limestone directly date its deposition (Fig. 2c), while the three volcanic tuffs stratigraphically below the limestone beds provide a check on the conformable nature of sediment deposition across the sequence (Fig. 3).

Radiolaria belonging to the *Pseudoalbaillella globosa* Zone to the *Follicucullus scholasticus* Zone of Wordian-Capitanian age were collected from the lower and middle parts of the Tsunemori Formation (Sano and Kanmera, 1991b; Tazawa et al., 2009; Wakita et al., 2018).

The fusulinids in the turbidites and in the limestone slump block in the Tsunemori Formation at the Shigeyasu Quarry are quite diverse and include schubertellids *Schubertella*, *Yangchienia*, *Codonofusiella*, *Kahlerina*~~,~~ and *Rauserella*, schwagerinids *Parafusulina* and *Chusenella* and verbeekinaceans *Lepidolina*, *Pseudodoliolina* and *Sumatrina* (Table 1). The taxonomic composition of fusulinids in the studied turbidites and slump block is generally consistent (Figs. 4-5) and therefore the age of the limestone turbidites/slump block and volcanoclastics in the quarry is the same within the resolution of fusulinids biostratigraphy, i.e. around ~~1~~ one ~~myrs~~ million years in this case (Davydov et al., 2018) (Table 1). The occurrence of species *Lepidolina shiraiwensis* Ozawa in the turbidites undoubtedly ~~suggests~~ constrains ~~the~~ and early Midian age ~~of~~ for the limestone turbidites and surrounding rocks (Leven, 1980; Kotlyar et al., 1989a). In the nearby Kaerimizu area of the Akiyoshi plateau, the carbonate succession ~~ended~~ ends within the *Colania douvillei* ~~zone~~ Zone (Ueno, 1992), but in places ~~extended~~ extends up to the *Lepidolina shiraiwensis* Zone, which is also defined in the area from the limestone blocks and calcareous sandstone (Kobayashi, 2012b, 2012a).

~~6.~~ 5. U-Pb ~~Geochronology~~ geochronology

Sample 10VD96 was the stratigraphically lowest sampled volcanic tuff within siliciclastic rocks at the Shigeyasu quarry, where the succession is overturned. Eight grains selected for CA-IDTIMS yielded dates ranging from 267.65 to 267.01 Ma; five of these analyses are concordant and equivalent with a weighted mean $^{206}Pb/^{238}U$ date of 267.46 ± 0.04 (0.14) [0.31] Ma (2s; MSWD = 1.90), which is interpreted as estimating the volcanic depositional age (Table 2, Fig. 6). Two analyses yielded resolvably older dates with a modified Thompson tau test, and are interpreted as representing ~~slightly older~~ inheritance, and a single analysis with an anomalously younger age is interpreted as the sole crystal in this study in which Pb-loss was not completely mitigated by chemical abrasion.

Sample 10VD95 from fifteen meters stratigraphically higher in the section was dated using ten single zircon grains; the five youngest analyses yielded a weighted mean ^{206}Pb/^{238}U date of 266.00 ± 0.04 (0.14) [0.31] Ma (2s; MSWD = 1.06), which is interpreted as estimating the volcanic depositional age (Table 2, Fig. 6). Another five grains produced older ages ranging from 266.25 to 269.85 Ma, and are attributed to inheritance.

Sample 10VD26 collected from a volcanic tuff 3.3 meters stratigraphically above sample 10VD95, and 1.7 meters below the base of the laminated limestone turbidite beds. All ten single zircons analyzed by CA-IDTIMS yielded concordant and equivalent isotope ~~ratios~~ ratios within their errors, with a weighted mean ^{206}Pb/^{238}U date of 265.81 ± 0.04 (0.13) [0.31] Ma (2s; MSWD = 1.05), which is interpreted as ~~estimating~~ the volcanic depositional age (Table 2, Fig. 6).

Samples 10VD25 and **10VD20** from the base and top of the laminated limestone turbidite bar in the Tsunemori Formation yielded indistinguishable radioisotopic ages. Ten single zircons from sample 10VD25 produced concordant and equivalent isotope ratios with a weighted mean ^{206}Pb/^{238}U date of 265.77 ± ± 0.03 (0.13) [0.31] Ma (2s; MSWD = 0.39), and ~~six of ten~~four of seven single grains from sample 10VD20 produced a weighted mean ^{206}Pb/^{238}U date of 265.76 ± 0.04(0.14)[0.31] Ma (2s; MSWD = ~~2.48~~1.60) (Table 2, Fig. 6). These dates demonstrate the expected increase in rock accumulation rate through the laminated limestone beds as compared to the underlying siliciclastic succession and affirm the effectively conformable nature of the siliciclastic-carbonate transition. The sequence of CA-IDTIMS radioisotopic ages also affirm the overturned orientation of the succession (Figs. 2-3), which is a common feature within the Tsunemori Formation (Wakita et al., 2018).

~~7.~~ 6. Discussion

6.1 Radioisotopic ages and sedimentation processes in the Tsunemori Formation.

The Tsunemori Formation at the Shigeyasu Quarry ~~possessed~~ possesses all of the features of a locally normal ~~sedimentation~~ sedimentary succession. Besides its overturned position in the ~~Quarry~~quarry, it is generally stratified throughout. The laterally traceable volcanic tuffs that were found in the Shigeyasu Quarry are marker beds of stratigraphic integrity, and could be preserved only in relatively ~~the~~ low energy environments. The presence of two volcanic tuff horizons of the same age (10VD20 and 10VD25) within the turbiditic limestone suggests normal sedimentation therein (Wakita et al., 2018), rather than ~~the~~ olistrosomal incorporation in a mélange ~~formation~~ environment (Sano and Kanmera, 1991b). ~~Consistent~~ The ~~consistent~~ regular succession of radioisotopic ages from 267.46± 0.04 at the bottom of the exposed part of the Tsunemori Formation (samples 10VD96) ~~towards~~ to 265.76 ± 0.04 Ma at the exposed top of the formation (Figs. 2-3), ~~and~~ combined with the consistent age of all fusulinids collected from limestone ~~fusulinids suggest~~ ~~the normal sedimentary processes of~~ provide the most compelling evidence for conformable sedimentation within the Tsunemori Formation at the Shigeyasu Quarry.

6.2 Midian Stage of the Tethyan provincial ~~Scale~~ time scale

The Midian Stage possesses a complicated history of establishment. Being proposed as a ~~Stage~~ stage equal to the *Yabeina-Lepidolina* fusulinids Genozone that is well known from Japan

(Toriyama, 1967), it was first ~~named~~ referred as the "Capitanian" Stage in the Tethys (Leven, 1975). ~~The~~ However the Genozone and "Capitanian" Stage designation ~~has mostly resulted~~ followed from compilation of the literature in Eastern Tethys without specific characterization of the stage boundaries (Leven, 1975). Furthermore, strong provincialism ~~T~~the lack of verbeekinids in the Capitanian of the type area in Texas (Dunbar and Skinner, 1937) has caused difficulty in fusulinid correlation of the Capitanian Stage of Texas outside of this region. Because of doubts on the exact correspondence of the *Yabeina-Lepidolina* fusulinids Genozone of the Tethys with the Capitanian Stage of Texas (Leven, 1980), a new Midian Stage equal to the Genozone was established with the potential type section in Transcaucasia. The base of the Midian Stage was first drawn at the base of the Arpa Formation in Transcaucasia without specific type section (Leven, 1980). ~~An alternative type section~~ The stratotype of the Stage was later proposed and the boundary defined at the base of ~~bed~~ Bed 33 in the Dzhagadzur section, Armenia, which coincided with the bottom of the Arpa Formation and with the base of the *Yangchienia thompsoni* local fusulinids zone (Kotlyar et al., 1989a). The Midian Stage in Transcaucasia is composed of massive limestone of the Arpa and Khachik Formations, totaling 350-450 m in thickness. Both the base of the Arpa and the top of Khachik Formations possess transitional contacts with the limestones below and above the Midian Stage (Kotlyar et al., 1989a). The Midian Stage in Transcaucasia comprises three fusulinids zones. The Arpa Formation is divided into the *Yangchienia thompsoni* (lower) and *Chusenella abichi* (upper) ~~zones~~ Zones (Kotlyar et al., 1989a). Small fusulinids *Reichelina*, *Dunbarula*, *Codonofusiella*, *Minojapanella (Wutuella)*, *Kahlerina* and *Pseudokahlerina* appear from the beginning of the Arpa Formation. No specific zone is proposed for the Khachik Formation, but in accordance with the fusulinid~~s~~ biota ~~content~~ in the formation (Kotlyar et al., 1989a) it could be named as the *Pseudofusulina solita -Neoschwagerina pinguis* ~~zone~~Zone. The latter~~se~~ two species have been described from Turkey in associated with typical upper Midian fusulinids *Yabeina opima* and small fusulinids such as *Reichelina*, *Dunbarula*, *Codonofusiella*, *Rauserella* and *Kahlerina* (Skinner, 1969; Kotlyar et al., 1989b). The Khachik Formation in Transcaucasia is conformably overla~~ying~~in by the Chanakhchi beds of Wuchiapingian age (Sahakyan et al., 2017).

The most confusing aspect in the designation of the Midian Stage is that no *Yabeina* or *Lepidolina* that originally were used for the concept of the stage designation (Leven, 1975) ~~are~~ occurr~~ing~~ in the type area in Transcaucasia. Rare *Neoschwagerina cheni* Sheng, 1956, *Verbeekina verbeeki* (Geinitz) and *V. furnishi* Skinner and Wilde are found in the underlying Gnishik Formation. A single specimen of *Neoschwagerina pinguis* Skinner has been found in bed 13 of the Khachik Formation at the type section of the Midian Stage, 122 meters above the base of the Stage (Kotlyar et al., 1989a). Similarly, a narrow bed with *Sumatrina vediensis* (Leven) has been reported approximately 70 m above the base of the Arpa Formation in the Vedi section (Leven, 1998). Although the type-section of the Midian Stage is lacking the indices *Yabeina* and *Lepidolina*, it is reasonably well correlated with sections in the East Tethys thanks to its stratigraphic position below the well-defined Wuchiapingian Stage of the IGTS (Kozur, 2005) in Transcaucasia, and to the abundant assemblage of small fusulinids ozawainellids and schubertellids, such as *Kahlerina*, *Pseudokahlerina*, *Dunbarula*, *Reichelina*, *Rauserella* and numerous species of advanced schwagerinids *Chusenella* that ~~are~~ occur within the entire Midian Stage (Kotlyar et al., 1989a; Leven, 1998). These genera and the species of the latter genus are very characteristic for the Midian deposits in Peri-Gondwana (Leven, 1998; Huang et al., 2009; Leven, 2009; Davydov and Arefifard, 2013) and Cathaysian blocks including South China (Sheng, 1963; Xiao et al., 1986). However, we cannot exclude that the lowermost part of the Midian Stage corresponds with the underlying *Yabeina* and *Lepidolina* ~~z~~Zones in Japan and South China.

~~Nevertheless, t~~The problem of precise correlation the base of the Midian Stage in Transcaucasia with the Capitanian Stage in Texas and elsewhere still exists, because of the limited characteristics of the Midian Stage in the type area, i.e. the lack of additional correlation tools, including geochemistry, paleomagnetism, and geochronology.

The Midian Stage ~~in~~ of Japan that equates to the well-studied fusulinids ~~of Genozone~~ *Yabeina-Lepidolina* Genozone (Toriyama, 1967), has become widely used since the Stage designation, although the position of its lower boundary in Japan was not certain. It was proposed (Leven, 1996) to include the *Neoschwagerina margaritae* ~~zone~~ Zone of Japan into the Midian Stage because of the appearance of small fusulinids *Reichelina*, *Codonofusiella*, Kahlerina in this zone, whereas the majority of Japanese micropaleontologists follow the strict definition of the stage in the sense ~~as~~ of First Appearance Datum (FAD) and Last Appearance Datum (LAD) of *Yabeina* and *Lepidolina* genera including *Lepidolina shiraiwensis*, *L. multiseptata* and *L. kumaensis* ~~zones~~ Zones (Ozawa, 1975; Ozawa et al., 1991; Kobayashi, 2012a) and *Yabeina globosa* ~~z~~Zone in the Jurassic terrane of Japan (Kobayashi, 2011b). Some Japanese paleontologists follow the suggestion of Leven (1996) and include the underlying *Yabeina-Lepidolina* Genozone, and the *Colania douvillei* ~~zone~~ Zone in the Akiyoshi Limestone into the Midian Stage (Nakazawa and Ueno, 2009).

6.3 Capitanian Stage in the type area in Texas

The Capitanian Stage in the traditional chronostratigraphic sense has been proposed in West Texas as an equivalent of the ammonoid *Timorites* Zone of earlier American literature (Glenister and Furnish, 1961). The lower boundary of the Capitanian Stage has conventionally been drawn at the base of the Hegler Member of the Bell Canyon Formation that is marking the base of the *Timorites* Zone. ~~Genus~~ The genus *Timorites* though has also been recovered from the preceding Manzanita Member of the upper Cherry Canyon Formation (Glenister et al., 1999). The Capitanian was also equated with the fusulinids *Polydiexodina* ~~zone~~Zone, which includes the provincial endemic genus *Polydiexodina*, advanced *Parafusulina*, and an abundant assemblage of small fusulinids such as *Rauserella*, *Reichelina*, *Parareichelina*, *Codonofusiella*, *Paradoxiella*, *Lantschichites*, and *Pseudokahlerina* (Dunbar and Skinner, 1937; Yang and Yancey, 2000; Nestell et al., 2006; Nestell and Nestell, 2006). The *Polydiexodina* ~~zone~~ Zone in the Glass Mountain of Texas is equated with the Vidrio and Altuda Formations (Dunbar and Skinner, 1937; Yang and Yancey, 2000) and with the Bell Canyon Formation (pre-Lamar Limestone) in the Guadalupe Mountains (Wilde, 1990).

The Capitanian (*sensu lato*) in this traditional sense seems to corresponds with the entire Midian Stage of the Tethyan Scale (Wardlaw, 2000; Menning et al., 2006) (Fig. 7). However the base of the International Capitanian Stage (*sensu stricto*), is defined in the upper part of the Pinery Limestone Member of the Bell Canyon Formation near the top of Nipple Hill (southeastern Guadalupe Mountains), at 4.5 meters in the outcrop section on the south side of the hill and coinciding with the FAD of the conodont *Jinogondolella postserrata* (Glenister et al., 1999). This ~~newly defined~~ base of the International Capitanian (*sensu stricto*) therefore, occurs much higher in the Guadalupian succession of West Texas than the traditional base of the

Capitanian (*sensu lato*). The Capitanian lower boundary is similarly shifted upwards from the base of Vidrio ~~Fm~~ Formation into the lower third of the Altuda Formation in the Glass Mountains~~.~~ (Fig. 7) (Rohr et al., 2000). In the latter region this is approximately **100 meters above** the traditional boundary ~~(estimated here as 3 Myrs)~~, whereas the total thickness of the entire Guadalupian in the Glass and Del Norte ~~mountains~~ Mountains is slightly over 300 meters (Wardlaw, 2000).

~~Once~~ As the ~~newly defined~~ current base of the International Capitanian Stage (*s. s.*) appears within the regional Midian Stage of the Tethyan ~~Scale~~ time scale (Fig. 7), the lower part of the Midian Stage in Tethys ~~become the part of~~ equites to the International Wordian Stage. This was quickly recognized by ~~the~~ fusulinids workers who found a typical assemblage of small fusulinids *Reichelina*, *Codonofusiella*, Kahlerina and *Pseudokahlerina* along with advanced *Neoschwagerina* and some *Yabeina* in the re-defined ~~International~~ upper Wordian Stage (Davydov, 1994; Stevens et al., 1997; Leven, 2001).~~,~~ Nonetheless, ~~but~~ most of the Japanese and Chinese fusulinid~~s~~ workers still consider the Midian Stage in ~~Eastern~~ eastern Tethys in the traditional sense, i.e. Capitanian (*s. l.*) (Ozawa and Kobayashi, 1990; Ozawa et al., 1991; Kobayashi, 2012a; Kofukuda et al., 2014; Zhang and Wang, 2018). Ammonoid workers also consider the Capitanian Stage in the traditional sense as the equivalent of *Timorites* ammonoid Genozone, because there is no opportunity to separate upper Wordian and lower Capitanian parts of the Genozone (Bogoslovskaya et al., 1995; Ehiro and Misaki, 2005; Leonova, 2018).

6.4 Biotic and radioisotopic correlation of the Midian ~~Stage of the Tethyan Scale~~ and the Capitanian Stages ~~of the International Geologic Time Scale~~.

Correlation of Midian Stage of the Tethyan ~~Scale~~ time scale with the IGTS has been difficult and controversial. Since its definition (Leven, 1980)~~,~~ and through the mid-1990s the Midian Stage ~~utilizing fusulinids and ammonoids~~ was correlated utilizing fusulinids and ammonoids with the Capitanian Stage (*s. l.*) Stage of Texas (Jin et al., 1997). Once the Capitanian was redefined and its lower boundary in Texas shifted upwards (Glenister et al., 1999), the fusulinid~~s~~ assemblages from the lower Capitanian (*s.l.*) now characterize the upper Wordian of the IGTS (Davydov, 1994; Kozur and Davydov, 1996; Stevens et al., 1997).

Nevertheless, in some regions this part of the succession~~s~~ has remained equated with the Capitanian (Menning et al., 2006; Nakazawa and Ueno, 2009; Kobayashi, 2011a, 2012a; Kofukuda et al., 2014). In Japan, the Guadalupian ~~succession~~ Series is divided into ~~a~~ ~~series~~several ~~of~~ fusulinids zones (Fig. 7). The lower Midian Stage in the Akiyoshi area in our opinion correlates with the upper part of *Colania douvelei-Neoschwagerina haydeni* ~~zone~~Zone, where the first *Kahlerina* appear (Nakazawa and Ueno, 2009; Kobayashi, 2012a). We suggest~~ing~~ naming this part of the *Colania douvelei-Neoschwagerina haydeni* ~~z~~Zone as the *Kahlerina* beds. Following upwards, the *Lepidolina shiraiwensis* ~~zone~~ Zone together with the *Kahlerina* ~~zone~~ Beds thus correlates with the upper Wordian of the IGTS (Fig. 7). The radioisotopic ages from the Manzanita bed of Texas (Bowring et al., 1998; Ramezani and Bowring, 2018) and from the *Lepidolina shiraiwensis* ~~zone~~ Zone of ~~Akasaka~~ Akiyoshi (this study) support such a correlation. This contrasts with and requires revision of the recent assignment of an uppermost Capitanian age for the *Lepidolina shiraiwensis* Zone in some recent publications (Zhang and Wang, 2018).

The *Kahlerina* beds and *Lepidolina shiraiwensis* ~~zone~~ Zone of ~~Japan~~ Akiyoshi and *Yabeina globosa* Zone of Akasaka consequently correlate with the Arpa Formation (lower Midian) of Transcaucasia (Kotlyar et al., 1988) (Kobayashi, 2011b), the lower Karasin Beds of ~~S-E~~ southeast Pamir (Chediya et al., 1986), and the *Yabeina inoyei* fusulinid ~~zone~~ Zone of South~~.~~ China (Mei et al., 1998). The Capitanian Stage (*s. s.*) of the IGTS correlates with the *Lepidolina multiseptata* and *L. kumaensis* ~~zones~~ Zones of Japan, the upper Midian Stage of the Tethyan ~~Scale~~time scale, the Khachik Formation of Transcaucasia, the upper Karasin Beds in the Pamirs where *Lepidolina* ex gr. *multiseptata* and *Yabeina opima* are found (Chediya et al., 1986; Kotlyar et al., 1989a), and the *Metadoliolina multivoluta-Lepidolina multiseptata* fusulinid ~~zone~~ Zone of South~~.~~ China (Fig. 7).

~~8.~~ 7. Conclusions~~.~~

The ~~succession~~sequence of radioisotopic ages and consistent age of all ~~collected from limestone~~ fusulinids suggest ~~the normal~~a conformable sedimentary ~~processes~~ succession ~~of~~ within the Tsunemori Formation at the Shigeyasu Quarry. The obtained radioisotopic, sedimentologic and biostratigraphic data of the Tsunemori Formation at the Shigeyasu Quarry and the presence of acidic volcanic tuffs ~~is~~are consistent with ~~the newly proposed model of the~~ a forearc basin or trench slope basin as the site of deposition ~~sedimentation site~~ for the ~~entire~~ Tsunemori Formation. ~~(Wakita et al., 2018).~~

The ~~siliclastic~~ mixed volcano-siliciclastic-carbonate succession w~~ith limestone turbidites and slump blocks~~ in the Tsunemori Formation at Shigeyasu Quarry, Japan, contains both fusulinids and tuffs with U-Pb zircon CA-IDTIMS radioisotopic ages that allow a robust correlation of the *Kahlerina* and *Lepidolina shiraiwensis* ~~zones~~ Zones of Japan to the lower Midian Stage of the Tethyan time scale, and to the upper Wordian Stage of the International Geologic Time Scale.

~~9.~~ Acknowledgements~~.~~

We would like to express our ~~attitude~~gratitude to Pacific Cement Limited Company and Mr. Takano Masinori from the company for permission to access the quarry. Prof. H. Sano provided many valuable suggestions and comments in the field and in the early version of the manuscript. This paper was completed with support from NSF grants EAR- 1124488 (to DVI and SMD). The work was supported by the Ministry of Education and Science of the Russian Federation contract No. 14.Y26.31.0029 in the framework of the Resolution No.220 of the Government of the Russian Federation. The funds from the subsidy allocated to Kazan Federal University for the state assignment #5.2192.2017/4.6 in the sphere of scientific activities and in part from the subsidy of the Russian Government to support the Program of Competitive Growth of Kazan Federal University among the World Leading Academic Centers (to DVI) are highly appreciated.

References

Angiolini, L., Zanchi, A., Zanchetta, S., Nicora, A., Vuolo, I., Berra, F., Henderson, C., Malaspina, N., Rettori, R., Vachard, D., Vezzoli, G., 2015. From rift to drift in South Pamir (Tajikistan): Permian evolution of a Cimmerian terrane. Journal of Asian Earth Sciences 102, 146–169.

Bogoslovskaya, M.F., Leonova, T.B., Shkolin, A.A., 1995. The Carboniferous-Permian boundary and ammonoids from the Aidaralash section, southern Urals. Journal of Paleontology 69, 288–301.

Bowring, S.A., Erwin, D.H., Jin, Y.G., Martin, M.W., Davidek, K., Wang, W., 1998. U/Pb zircon geochronology and tempo of the end-Permian mass extinction. Science 280, 1039–1045.

Chediya, I.O., Bogoslovskaya, M.F., Davydov, V.I., Dmitriyev, V.Y., 1986. Fuzulinidy i ammonoidey v stratotipe kubergandinskogo yarusa (Yugo-Vostochnyy Pamir). Fusulinids and ammonoids in the stratotype of the Kubergandy Stage; southeastern Pamirs. Ezhegodnik Vsesoyuznogo Paleontologicheskogo Obshchestva 29, 28–53.

Cohen, K.M., Finney, S.C., Gibbard, P.L., Fan, J.X., 2013. The ICS International Chronostratigraphic Chart. Episodes 36, 199–204.

Davydov, V.I., 1994. Murgabian-Midian fusulinid zonation and the problem of correlatingthe Murgabian/Midian boundary in a global scale. Abstracts with program International Symposium on Permian Stratigraphy, Environments & Resources with International Meetings of Pangea Project GSSP, IGSP 306 & 359, 5–6.

Davydov, V.I., Arefifard, S., 2013. Middle Permian (Guadalupian) fusulinid taxonomy and biostratigraphy of the mid-latitude Dalan Basin, Zagros, Iran and their applications in paleoclimate dynamics and paleogeography. Geoarabia 18 (2), 17–62.

Davydov, V.I., Biakov, A.S., Isbell, J.L., Crowley, J.L., Schmitz, M.D., Vedernikov, I.L., 2016. Middle Permian U–Pb zircon ages of the “glacial” deposits of the Atkan Formation, Ayan-Yuryakh anticlinorium, Magadan province, NE Russia: Their significance for global climatic interpretations. Gondwana Research 38, 74–85.

Davydov, V.I., Biakov, A.S., Schmitz, M.D., Silantiev, V.V., 2018. Radioisotopic calibration of the Guadalupian (middle Permian) series: Review and updates. Earth-Science Reviews 176, 222–240.

Dunbar, C.O., Skinner, J.W., 1937. Permian Fusulinidae of Texas. The University of Texas Bulletin 3701, 517–825.

Ehiro, M., Misaki, A., 2005. Middle Permian ammonoids from the Kamiyasse-Imo district in the Southern Kitakami Massif, Northeast Japan. Paleontological Research 9 (1), 1–14.

Glenister, B.F., Furnish, W.M., 1961. The Permian ammonoids of Australia. Journal of Paleontology 35 (4), 673–736.

Glenister, B.F., Wardlaw, B.R., Lambert, L.L., Spinosa, C., Bowring, S.A., Erwin, D.H., Menning, M., Wilde, G.L., 1999. Proposal of Guadalupian and Component Roadian, Wordian and Capitanian Stages as International Standards for the Middle Permian Series. Permophiles 34, 3–11.

Gradstein, F.M., Ogg, J.G., Schmitz, M.D., Ogg, G. (Eds.), 2012. *The Geologic Time Scale 2012.* Elsevier, Amsterdam, 1176 p.

Hara, H., Hirano, M., Kurihara, T., Takahashi, T., Ueda, H., 2018. Permian arc evolution associated with Panthalassa subduction along the eastern margin of the South China block, based on sandstone provenance and U–Pb detrital zircon ages of the Kurosegawa belt, Southwest Japan. Journal of Asian Earth Sciences 151, 112–130.

Henderson, C., Davydov, V.I., Wardlaw, B.R., 2012. The Permian Period, in: Gradstein, F.M., Ogg, J.G., Schmitz, M.D., Ogg, G. (Eds.), The Geologic Time Scale 2012, vol. 2. Elsevier, Amsterdam, pp. 653–679.

Huang, H., Jin, X., Shi, Y., Yang, X., 2009. Middle Permian western Tethyan fusulinids from southern Baoshan Block, western Yunnan, China. J. Paleontol. 83 (06), 880–896.

Jin, Y., Wardlaw, B.R., Gleinster, B.F., Kotlyar, G.V., 1997. Permian chronostratigraphic subdivisions. Episodes 20 (1), 10–15.

Kanmera, K., 1974. Paleozoic and Mesozoic geosynclinal volcanism in the Japanese Islands and associated chert sedimentation. Special Publication - Society of Economic Paleontologists and Mineralogists 19, 161–173.

Kanmera, K., Nishi, H., 1983. Accreted ocean reef complex in southwest Japan.: In: Hashimoto, M., Ueda, S. (Eds.), Accretion Tectonics in the Circum-Pacific regions. Terra Scientific Publishing Company, Tokyo.

Kobayashi, F., 2011~~a~~. Permian fusuline faunas and biostratigraphy of the Akasaka Limestone (Japan). Revue de Paléobiologie 30 (2), 431–574.

~~Kobayashi, F., 2011b. Permian fusuline faunas and biostratigraphy of the Akasaka Limestone (Japan). Revue de Paléobiologie 30 (2), 431–574.~~

Kobayashi, F., 2012a. Comparative study of the Capitanian (late Guadalupian) foraminiferal faunas in the *Lepidolina shiraiwensis* ~~zone~~ Zone of the Akiyoshi limestone group, SW Japan. The Journal of Foraminiferal Research 42 (1), 82–101.

~~Kobayashi, F., 2012b. COMPARATIVE STUDY OF THE CAPITANIAN (LATE GUADALUPIAN) FORAMINIFERAL FAUNAS IN THE LEPIDOLINA SHIRAIWENSIS ZONE OF THE AKIYOSHI LIMESTONE GROUP, SW JAPAN. The Journal of Foraminiferal Research 42 (1), 82–101.~~

Kobayashi, F., 2012c. Late Paleozoic ~~Foraminifers~~ foraminifers from l~~L~~imestone ~~Blocks~~ blocks and ~~Fragments~~ fragments of the Permian Tsunemori Formation and ~~Their~~ their ~~Connection~~ connection to the Akiyoshi Limestone Group, Southwest Japan. Paleontological Research 16 (3), 219–243.

Kofukuda, D., Isozaki, Y., Igo, H., 2014. A remarkable sea-level drop and relevant biotic responses across the Guadalupian–Lopingian (Permian) boundary in low-latitude mid-Panthalassa: Irreversible changes recorded in accreted paleo-atoll limestones in Akasaka and Ishiyama, Japan. Journal of Asian Earth Sciences 82, 47–65.

Kotlyar, G.V., Chediya, I.O., Kropacheva, G.S., Pronina, G.P., Rostovtsev, K.O., 1988. Regional biostratigraphic scales and sections of the Transcaucasian Permian deposits. Sovetskaya Geologiya 1988 (2), 47–57.

Kotlyar, G.V., Zakharov, Y.D., Kropacheva, G.S., Pronina, G.P., Chedija, I.O., Burago, V.I., 1989a. Evolution of the latest Permian Biota. Midian regional stages in the USSR. Nauka, Leningrad.

Kotlyar, G.V., Zakharov, Y.D., Kropacheva, G.S., Pronina, G.P., Chediya, I.O., Burago, V.I., 1989b. Evolution of the latest Permian biota. Midian regional stage in the USSR. Nauka (In Russian), Leningrad.

Kozur, H., 2005. Pelagic uppermost Permian and the Permian-Triassic boundary conodonts of Iran. Part 2. Investigated sections and evaluation of the conodont faunas. Hallesches Jahrb. Geowiss., B Beiheft 19, 49–86.

Kozur, H., Davydov, V.I., 1996. The importance of the Permian of the Sosio Valley (Western Sicily, Italy) for Guadalupian Stratigraphy. Abstracts and proceedings of the Second International Guadalupian Symposium, 11–15.

Kozur, H., Davydov, V.I., Kotlyar, G.V., 1994. Preliminary report on the Permian conodont fauna of Darvas and SE Pamir and its importance for the Permian time scale. AND ITS IMPORTANCE FOR THE PERMIAN TIME SCALE. Permophiles (24), 13–15.

Leonova, T.B., 2018. Permian ammonoid biostratigraphy, in: Lucas, S.G., Shen, S. (Eds.), The Permian Times. Special Publications, pp. 185–203.

Leven, E.J., 1980. Explonatory notes to the Stratigraphicn Scale of the Permian deposits of Tethyan Realm. Leningrad, VSEGEI Institute, 1-51 (In Russian).

Leven, E.J., 1998. Permian fusulinid assemblages and stratigraphy of the Transcaucasia. Rivista Italiana di Paleontologia e Stratigrafia 104 (3), 299–328.

Leven, E.J., 2001. On ~~Possibility~~ possibility of ~~Using~~ using the ~~Global~~ global Permian Stage ~~S~~scale in the Tethyan ~~Region~~region. Stratigraphy and Geological Correlation 9 (2), 118-131.

Leven, E.J., 2009. The Upper Carboniferous (Pennsylvanian) and Permian of the Western Tethys: fusulinids, stratigraphy, biogeography. GEOS, Moscow, 246 (In Russian).

Leven, E.Y., 1967. Stratigrafiya i fuzulinidy permskikh otlozheniy Pamira; stratigraphy and fusulinides of the Pamirs Permian deposits. Trudy - Geologicheskiy Institut (Moskva) 167, 215.

Leven, E.Y., 1975. Yarusnaya shkala permskikh otlozheniy Tetisa. The stage scale of the Permian deposits of the Tethys. Byulleten' Moskovskogo Obshchestva Ispytateley Prirody, Otdel Geologicheskiy 50 (1), 5–21.

Leven, E.Y., 1996. Midiyskiy yarus permi i yego granitsy. Permian Midian stage and its boundaries. Stratigrafiya, Geologicheskaya Korrelyatsiya 4 (6), 20–31.

Mattinson, J.M., 2005. Zircon U-Pb chemical abrasion ("CA-TIMS") method: combined annealing and multi-step partial dissolution analysis for improved precision and accuracy of zircon ages. Chemical Geology 220, 47–66.

Mei, S., Jin, Y.G., Wardlaw, B.R., 1998. Conodont succession of the Guadalupian-Lopingian boundary strata in Laibin of Guangxi, China and West Texas, USA. Palaeoworld (9).

Menning, M., Alekseev, A.S., Chuvashov, B.I., Davydov, V.I., Devuyst, F.X., Forke, H.C., Grunt, T.A., Hance, L., Heckel, P.H., Izokh, N.G., Jin, Y.G., Jones, P.J., Kotlyar, G.V., Kozur, H.W., Nemyrovska, T.I., Schneider, J.W., Wang, X.D., Weddige, K., Weyer, D., Work, D.M., 2006. Global time scale and regional stratigraphic reference scales of central and west Europe, east Europe, Tethys, south China, and North America as used in the Devonian-Carboniferous-Permian Correlation Chart 2003 (DCP 2003). Palaeogeography, Palaeoclimatology, Palaeoecology 240 (1-2), 318–372.

Nakazawa, T., Ueno, K., 2009. Carboniferous-Permian long-term sea-level change inferred from Panthalassan oceanic atoll stratigraphy. Palaeoworld 18 (2-3), 162–168.

Nestell, G.P., Nestell, M.K., 2006. Middle Permian (Late Guadalupian) foraminifers from Dark Canyon, Guadalupe Mountains, New Mexico. Micropaleontology 52 (1), 1–50.

Nestell, M.K., Nestell, G.P., Wardlaw, B.R., Sweatt, M.J., 2006. Integrated biostratigraphy of foraminifers, radiolarians and conodonts in shallow and deep water Middle Permian (Capitanian) deposits of the “Rader slide”, Guadalupe Mountains,West Texas. Stratigraphy 3 (3), 161–194.

Okawa, H., Shimojo, M., Orinashi, Y., Yamamoto, K., Hirata, T., Sano, S.-i., Isozaki, Y., Kouchi, Y., Yanai, S., Otoh, S., h, 2013. Detrital zircon geochronology of the Silurian–lower Cretaceous continuous succession of the South Kitakami belt, Northeast Japan. Memoir of the Fukui Prefectural Dinosaur Museum 12, 35–78.

Ozawa, T., 1975. Evolution of Lepidolina multiseptata; Permian foraminifer, in East Asia. Memoirs of the Faculty of Science, Kyushu University, Series D: Geology 23 (2), 117–164.

Ozawa, T., Kobayashi, F., 1990. Carboniferous to Permian Akiyoshi Limestone Group. In : Organization Committee Benthos '90 (ed.), Fossils and recent benthic foraminifera in some selected regions in Japan. Guidebook for field trips, 4th International Symposium on Benthic Foraminifera, E1-E31.

Ozawa, T., Kobayashi, F., Watanabe, K., 1991. Biostratigraphic zonation of Late Carboniferous to Early Permian sequence of the Akiyoshi Limestone Group, Japan and its correlation with reference sections in the Tethyan region. Proceedings of the International Symposium on Shallow Tethys 3, 327–341.

Ramezani, J., Bowring, S.A., 2018. Advances in numerical calibration of the Permian timescale based on radioisotopic geochronology, in: Lucas, S.G., Shen, S. (Eds.), The Permian Timescales~~s~~. Special Publication - Geological Society of London 480 ~~Special Publications~~, ~~pp.~~ 51–60.

Rohr, D., Wardlaw, B.R., Rudine, S.F., Hafeef, M., Hall, A.J., Grant, R.E., 2000. Guidebook to the Guadalupian Symposium., in: Wardlaw, B.R., Grant, R.E., Rohr, D.M. (Eds.), The Guadalupian Symposium. Smithsonian Contribution to the Earth Sciences, No 32, vol. 32. Smithsonian Institute Press, Washington, DC, pp. 5–36.

Sahakyan, L., Baud, A., Grigoryan, A., Friesenbichler, E., Richoz, S. (Eds.), 2017. The Permian-Triassic transition in southern Armenia~~THE PERMIAN-TRIASSIC TRANSITION IN SOUTHERN ARMENIA~~. IGCP 630 Field Workshop in Armenia. Institute of Geological Sciences, National Academy of Sciences of Armenia, Yerevan, 54 pp.

Sano, H., Kanmera, K., 1991a. Collapse of ancient oceanic reef complex; what happened during collision of Akiyoshi reef?: Limestone breccias, redeposited limestone debris and mudstone injections. Chishitsugaku Zasshi = Journal of the Geological Society of Japan 97 (4), 297–309.

~~Sano, H., Kanmera, K., 1991b. Collapse of ancient oceanic reef complex; what happened during collision of Akiyoshi reef?: Limestone breccias, redeposited limestone debris and mudstone injections. Chishitsugaku Zasshi = Journal of the Geological Society of Japan 97 (4), 297–309.~~

Sano, H., Kanmera, K., 1991c. Collapse of ancient oceanic reef complex; what happened during collision of Akiyoshi reef?: Sequence of collisional collapse and generation of collapse products. Chishitsugaku Zasshi = Journal of the Geological Society of Japan 97 (8), 631–644.

Sheng, J.-z., 1963. Permian fusulinids of Kwangsi, Kueichow and Szechuan.: Palaeontologica Sinica, vol. 149, New Series B, No 10, 111-247. Schience Press, Peking.

Skinner, J.W., 1969. Permian foraminifera from Turkey. University of Kansas Paleontological Contributions, Paper 36, 14 p.

Stevens, C.H., Davydov, V.I., Bradley, D.C., 1997. Permian Tethyan Fusulinina from the Kenai Peninsula, Alaska. Journal of Paleontology 71 (6), 985–994.

Tazawa, J.-i., Fujikawa, M., Ota, Y., 2009. Permian brachiopods from the Tsunemori Formation of the Akiyoshi area, southwest Japan: Fossil evidence for the accretion site of the Akiyoshi Terrane. Jour. Geol. Soc. Japan 115 (4), 168–176.

Toriyama, R., 1967. The fusulinacean zones of Japan. Memoirs of the Faculty of Science, Kyushu University, Series D, Earth and Planetary Sciences 18 (1), 35–260.

Ueno, K., 1992. Verbeekinid and Neoschwagerinid fusulinaceans from the Akiyoshi Limestone Group above the *Parafusulina kaerimizensis* Zone, Southwest Japan. Transactions and Proceedings of the Palaeontological Society of Japan. New Series 165, 1040–1069.

Wakita, K., 2013. Geology and tectonics of Japanese islands: A review – The key to understanding the geology of Asia. Journal of Asian Earth Sciences 72, 75–87.

Wakita, K., Yoshida, R., Fushimi, Y., 2018. Tectonic setting for Tsunemori Formation in the Permian accretionary complex of the Akiyoshi Belt, Southwest Japan. Heliyon 4 (12), e01084.

Wardlaw, B.R., 2000. Guadalupian Conodont Biostratigraphy of the Glass and Del Norte Mountains, in: Wardlaw, B.R., Grant, R.E., Rohr, D.M. (Eds.), The Guadalupian Symposium. Smithsonian Contribution to the Earth Sciences, No 32. Smithsonian Institute Press, Washington, DC, pp. 37–88.

Wilde, G.L., 1990. Practical fusulinid zonation: the species concept; with Permian basin emphasis. West Texas Geological Society 29, 5–34.

Wu, Q., Ramezani, J., Zhang, H., Wang, T., Yuan, D., Mu, L., Zhang, Y., Li, X., Shen, S., 2017. Calibrating the Guadalupian Series (Middle Permian) of south China. Palaeogeography, Palaeoclimatology, Palaeoecology 466, 361–372.

Xiao, W., Wang, H., Zhang, L., Dong, W.-l., 1986. Early permian stratigraphy and faunas in Southern Guizhou. The People's Publishing House of Guizhou, Guizhou, China, 1-364 (In Chinese).

Yang, Z., Yancey, T.E., 2000. Fusulinid Biostratigraphy and Paleontology of the Middle Permian (Guadalupian) Strata of the Glass Mountains and Del Norte Mountains, West Texas, in: Wardlaw, B.R., Grant, R.E., Rohr, D.M. (Eds.), The Guadalupian Symposium. Smithsonian Contribution to the Earth Sciences, No 32. Smithsonian Institute Press, Washington, DC, pp. 185–260.

Zhang, X., Takeuchi, M., Ohkawa, M., Matsuzawa, N., 2018. Provenance of a Permian accretionary complex (Nishiki Group) of the Akiyoshi Belt in Southwest Japan and Paleogeographic implications. Journal of Asian Earth Sciences.

Zhang, Y.-C., Wang, Y., 2018. Permian fusuline biostratigraphy, in: Lucas, S.G., Shen, S. (Eds.), The Permian Times. Special Publications, pp. 253–288.

Figure and Tables Captures

Figure 1. Paleogeographic and tectonic maps. (**A**) Middle Permian global paleogeography with the main regions discussed in this paper; (**B**) Regional tectonic map of southern Japan, modified from ~~(~~Wakita~~,~~ (2013).

Figure 2. **Shigeyasu Quarry**: **a**, Google Earth image of Shigeyasu Quarry, red line shows collection site; **b**, general panorama of studied site; **c**, volcanic ash (10VD20) within the laminated limestone. Stratification is well expressed ~~at the of~~ within the Shigeyasu Quarry cut.

Figure 3. Stratigraphic log of the succession in Shigeyasu Quarry and position of the collected samples. Note, that the succession there is overturned. All scale bars on fusulinids are 1mm. The entire set of the radioisotopic ages attributes can be seen in Table 2.

Figure 4. Fusulinid assemblage from turbiditic bed (samples 10VD20-10VD23). 1, *Schubertella ovalis* Kobayashi; 2, *Yangchienia*? sp.; 3, *Kahlerina* sp.; 4-5, *Chusenella altinensis* Ross; 6, *Chusenella otai* (Nogami); 7-12, *Lepidolina shiraiwensis* (Ozawa); 13, *Sumatrina longissima* Deprat. All scale bars are 1mm.

Figure 5. Fusulinid assemblage from slump block (sample 10VD98). 1, *Codonofusiella* sp.; 2, boultoniids; *Kahlerina ampla* Han; 4-7, *Kahlerina nautiloidea* Sosnina; 8, *Kahlerina* sp.; 9, *Rauserella* ex gr. *ellipsoidalis* Sosnina; 10, *Chusenella altinensis* Ross; 11, *Chusenella otai* (Nogami); 12-15, *Lepidolina shiraiwensis* (Ozawa); 16, *Sumatrina longissima* Deprat; 17, *Pseudodoliolina ozawai* Yabe and Hanzawa. All scale bars are 1mm.

Figure 6. U-Pb concordia diagrams illustrating results of single grain chemical abrasion ID-TIMS analysis for each dated tuff samples from Shigeyasu Quarry, volcano-siliciclastic succession of the Akiyoshi Plateau, southwest Japan. Grey band represents the error envelope on the concordia curve based upon the decay constants and errors of Jaffey et al. (1975). Analyses accepted in weighted mean calculations are illustrated by filled translucent ellipses; analyses discarded as influenced by inheritance or Pb-loss are illustrated as open ellipses. All accepted analyses are concordant within the decay constant uncertainties.

Figure 7. Biostratigraphic and radioisotopic correlation of the Guadalupian of **Shigeyasu Quarry** with ~~the global~~ major global sections~~. Data in~~: **Texas** – from (Glenister et al., 1999; Wardlaw, 2000; Yang and Yancey, 2000; Nestell et al., 2006; Nestell and Nestell, 2006); ~~in~~ **Japan** ~~from~~ (Ueno, 1992; Nakazawa and Ueno, 2009; Kobayashi, 2012a); ~~in~~ **Transcaucasia** ~~from~~ (Kotlyar et al., 1989a; Leven, 1998); ~~in~~ **Pamirs** ~~from~~ (Leven, 1967; Chediya et al., 1986; Kozur et al., 1994; Angiolini et al., 2015) and our own data; in ~~S.~~South China from (Mei et al., 1998; Wu et al., 2017).

Table 1. Fusulinid~~s~~ taxonomic composition of the studied limestone samples.

Table 2. Zircon IDTIMS U-Pb isotopic data

Highlights

New CA-IDTIMS radioisotopic ages were obtained from the lower Midian Stage of the Akiyoshi Plateau, Japan

Tuffs occur within limestone turbidite beds containing Early Midian fusulinids of the Tethyan province

The lower Midian correlates with upper Wordian of the Permian International Geologic Time Scale.

The obtained data from the Tsunemori Fm consistent with the newly proposed model of the forearc basin

High-precision radioisotopic ages for the lower Midian (upper Wordian) Stage of the Tethyan time scale, Shigeyasu Quarry, Yamaguchi Prefecture, Japan

Davydov, V. I.[1,2], and Schmitz, M. D.[1]

[1]Department of Geosciences, Boise State University, Boise, ID, 83725, USA (vdavydov@boisesate.edu)

[2] Kazan Federal University, 18 Kremlyovskaya St., Kazan, Republic of Tatarstan 420008, Russia

* Corresponding author: vdavydov@boisestate.edu

Abstract.

Global correlation of strata to the Guadalupian Series (Permian Period) of the International Geologic Time Scale remains provisional due to a lack of the sufficient biostratigraphically constrained radioisotopic ages. Five new high-precision U-Pb radioisotopic ages were obtained from tuffs in the lower Midian (upper Wordian) volcano-siliciclastic succession of the Akiyoshi Plateau, southwestern Japan. Two undisturbed and continuous tuffs occur within fusulinid-bearing laminated limestone turbidites with precise biostratigraphic control. The *Colania douvillei* and *Lepidolina shiraiwensis* fusulinid Zones in the Akiyoshi succession provide an early Midian age in the Tethyan provincial time scale. The range of ages (267.46 ± 0.04 Ma to 265.76 ± 0.03 Ma) over 25 m of section including the limestone turbiditic beds suggest that this lower Midian Stage of the Tethyan time scale is correlated with the upper Wordian Stage of the International Geologic Time Scale. The sedimentologic, bio- and geochronologic data affirm the effectively conformable nature of the siliciclastic-carbonate succession of the Tsunemori Formation at the Shigeyasu Quarry, and the presence of acidic volcanic tuffs are consistent with a forearc basin or trench slope basin depocenter for the Tsunemori Formation.

Key words: Guadalupian; Permian; zircon; CA-IDTIMS, fusulinid; biostratigraphy

1. Introduction

Significant progress has been made in the last decade on the radioisotopic calibration of the International Geologic Time Scale (IGTS) (Gradstein et al., 2012; Cohen et al., 2013), yet some parts of the time scale are still calibrated only provisionally. This is particularly true for the late Cisuralian (post Artinskian) and Guadalupian Epochs of the Permian (280-265 Ma), where just a few reliable high-precision U-Pb ages exist (Henderson et al., 2012). This part of the Permian Time Scale that is calibrated only with biostratigraphic scaling requires further geochronologic improvement. The paleobiogeographic provinciality and the lack of the radioisotopic calibration of this part of the scale make the correlation of Guadalupian Series and Stages in the type region with the rest of the world difficult. The only calibrating radioisotopic age in the entire Guadalupian in the type area is from a volcanic ash between the Hegler and Pinery limestone members of the Bell Canyon Formation at Nipple Hill, Guadalupe Mountains National Park, Texas. The ash is 6 to 8 cm thick and lies 2 m above the top of the Hegler Member, within the undifferentiated Bell Canyon Formation, and 20 m below the base of the *Jinogondolella postserrata* conodont Zone and the base of the Capitanian Stage (Bowring et al., 1998). The original legacy age of 265.3 ± 0.2 Ma for this volcanic tuff was recently revised using the chemical abrasion isotope dilution thermal ionization mass spectrometry (CA-IDTIMS) method to 265.46 ± 0.27 Ma (Ramezani and Bowring, 2018).

Several CA-IDTIMS radioisotopic ages were recently published from the base of Kuhfengian in South China (Wu et al., 2017) and from the analogues of the Roadian (Russian-Omolonian and Olynian Regional Stages in N-E of Russian) and Capitanian (Gizhigian Regional Stage) in N-E of Russia (Davydov et al., 2016; Davydov et al., 2018). The latter publication suggests a new calibration of the entire Guadalupian Epoch and proposes the extension of the base of the Roadian down to 277 Ma and the Wordian down to 271 Ma. The EARTHTIME isotope dilution tracer was utilized in all of these studies, which aids in the direct comparison of the dates from Texas, Russia and South China.

The correlation between the type section of the Guadalupian Epoch in Texas and the Tethyan time scale remains quite controversial (Davydov et al., 2018). Specifically, we do not know the exact analogues of all three stages of the Guadalupian in the Tethyan time scale. The report in this study of new high-precision U-Pb zircon ages for the lower Midian Stage of Japan is one step towards that correlation. The fusulinid fauna within the limestone turbidites and limestone slump blocks intercalated with the dated volcanic ashes are consistently early Midian in age and therefore can refine the maximum age of that stage in the Tethyan time scale and its correlation to an upper Wordian Stage in the IGTS.

2. Geological setting

Samples for the present study were collected at Shigeyasu Quarry, in rocks of the Akiyoshi Belt, which is distributed across several isolated areas of the Inner Zone of Southwestern Japan, extending into the western margin of the Hida Belt (Wakita, 2013). The Akiyoshi Belt forms a Permian accretionary complex (Fig. 1) composed of sandstone, mudstone, conglomerate, siliceous shale, felsic tuff, chert, limestone and basalt. The Permian Akiyoshi accretionary complex is divided into two units, which show similar ages but distinctly different dominant lithologies: a limestone-rich unit consisting of several large limestone plateaus that belong to the Akiyoshi Limestone Group, and a second unit that is composed mainly of siliciclastic successions with minor volcanic components, named the Tsunemori Formation. Both units formed by continuous sedimentation through the same period (Sano and Kanmera, 1991a; Tazawa et al., 2009). Many components of this belt are unmetamorphosed and the limestone within the belt is famous for its well preserved and diverse fauna (Toriyama, 1967). The Tsunemori Formation is unconformably overlain by Triassic shallow marine to non-marine sedimentary rocks of the Mine Group.

The Akiyoshi Limestone Group covers almost the whole area of the Akiyoshi Plateau in the central part of Yamaguchi Prefecture, southwest Japan. The Akiyoshi Limestone Group is a reefal limestone on a seamount in the Panthalassan Ocean (Kanmera and Nishi, 1983), and is one of the most complete and continuous carbonate successions in the Panthalassa region, ranging from Early Carboniferous to Middle Permian in age (Toriyama, 1967).

The Tsunemori Formation along the marginal parts of the western Akiyoshi-dai Plateau, southwest Japan, is described as a sequence of broken limestone, limestone breccia, and scaly mudstone (Sano and Kanmera, 1991b), designated as evidence of melange formation caused during subduction and accretion. The broken limestone is characterized by penetrative and pervasive destruction of skeletal grains and primary sedimentary fabrics. Late Visean to Midian foraminifera from the same depositional period as the entire Akiyoshi Limestone Group are identified in the broken limestone, but with no orderly stratigraphic succession (Sano and Kanmera, 1991a; Tazawa et al., 2009; Kobayashi, 2012a). The Tsunemori Formation according the first authors is a trench deposit, with the Akiyoshi Limestone accreted as an exotic block sometime during Middle to Late Permian time, based upon radiolarian biostratigraphy (Sano and Kanmera, 1991c).

An alternative model for Tsunemori Formation sedimentation and depositional setting has been proposed recently in the territory west of the Akiyoshi-dai Plateau, that includes the area of our study (Wakita et al., 2018). A conformable succession of mudstone and mudstone-dominant turbidite with very thin layers of sandstone or siltstone and rare horizons of calcarenite and limestone breccia is documented there. No fissility or scaly cleavage is recognized in the mudstone and pebbly mudstone of the Tsunemori Formation (Wakita et al., 2018). The lack of penetrative deformation is inconsistent with sedimentary formations deposited at the trench, and rather suggests a forearc basin or trench slope basin as the sedimentation site for the Tsunemori Formation (Wakita et al., 2018). Our brief field investigation of the Tsunemori Formation at Shigeyasu Quarry documents that the formation is faulted and overturned, but generally stratified (Fig. 2). We found three types of limestone within the Tsunemori Formation: 1) rare horizons of clastic limestone interbedded with debris flows and turbidites; 2) fully isolated blocks (2x3 m) of limestone (10VD98), wholly embedded in mudstone, i.e. slump block; 3) laminated limestone turbidite (10VD21, 22,23) (Figs. 2-3). Fusulinid samples from all three types of the limestone possessed the same early Midian Stage fauna.

Acidic volcanism in the late Guadalupian and Lopingian of Japan in general, and specifically volcanic rocks in the upper Guadalupian of the Akyioshi Group have long been recognized (Kanmera, 1974). Recent provenance and petrologic studies confirm the presence of a volcanic arc system near the Akiyoshi terrane during the entire Permian (Okawa et al., 2013; Hara et al., 2018; Zhang et al., 2018).

3. Materials and methods

Five samples of volcanic tuff and four samples of limestone were collected in the succession of the lower Tsunemori Formation exposed along the north-east to south-west edge of Shigeyasu Quarry (Fig. 2). The samples for radioisotopic study were collected from bentonitic volcanic tuff layers that occur within the lower part of the succession (Fig. 3). Three horizons were sampled from within siliciclastic beds 1.7, 5, and 20 meters below the base of a prominent bar of laminated limestone turbidite beds (samples 10VD26, 10VD95, and 10VD96, respectively). Two tuff samples were collected from within the laminated limestone turbidite beds near their base and top (samples 10VD25 and 10VD20 respectively), thus bracketing several of the fusulinid samples (Figs. 2-3). All tuffs are laterally traceable within the exposure of the Tsunemori Formation at the quarry.

All tuffs were processed with standard procedures including ultrasonic disaggregation and concentration (Hoke et al., 2014), Franz magnetic separation, heavy liquid separation, and hand picking. All samples yielded hundreds of sharply facetted, prismatic zircon grains (Figs. 2-3). The procedure and approaches associated with chemical-abrasion isotope dilution thermal ionization mass-spectrometry (CA-IDTIMS) method have been recently described in detail by Davydov et al. (2018). CA-IDTIMS dates are reported with weighted mean uncertainties given as ± X/Y/Z, where X is the 2σ analytical uncertainty, Y is the combined analytical and tracer uncertainty (value given in parentheses), and Z is the combined analytical, tracer, and decay constant uncertainty [value given in brackets]. The limestone samples were sliced into plates and fifty-one thin-sections with oriented fusulinid sections were prepared.

4. Biostratigraphic results

We acknowledge that fusuilinid-bearing limestone turbidites (debris flows) are allochthonous with respect to the deeper water syn-sedimentary siliciclastic rocks, and thus their biostratigraphic constraints would generally only constrain the maximum depositional age of such a stratigraphic succession. In this case, however, volcanic ash beds at the base and within the laminated turbiditic limestone directly date its deposition (Fig. 2c), while the three volcanic tuffs stratigraphically below the limestone beds provide a check on the conformable nature of sediment deposition across the sequence (Fig. 3).

Radiolaria belonging to the *Pseudoalbaillella globosa* Zone to the *Follicucullus scholasticus* Zone of Wordian-Capitanian age were collected from the lower and middle parts of the Tsunemori Formation (Sano and Kanmera, 1991b; Tazawa et al., 2009; Wakita et al., 2018). The fusulinids in the turbidites and in the limestone slump block in the Tsunemori Formation at the Shigeyasu Quarry are quite diverse and include schubertellids *Schubertella*, *Yangchienia*, *Codonofusiella*, *Kahlerina* and *Rauserella*, schwagerinids *Parafusulina* and *Chusenella* and verbeekinaceans *Lepidolina*, *Pseudodoliolina* and *Sumatrina* (Table 1). The taxonomic composition of fusulinids in the studied turbidites and slump block is generally consistent (Figs. 4-5) and therefore the age of the limestone turbidites/slump block and volcanoclastics in the quarry is the same within the resolution of fusulinid biostratigraphy, i.e. around one million years in this case (Davydov et al., 2018) (Table 1). The occurrence of species *Lepidolina* *shiraiwensis* Ozawa in the turbidites undoubtedly constrains an early Midian age for the limestone turbidites and surrounding rocks (Leven, 1980; Kotlyar et al., 1989). In the nearby Kaerimizu area of the Akiyoshi plateau, the carbonate succession ends within the *Colania douvillei* Zone (Ueno, 1992), but in places extends up to the *Lepidolina shiraiwensis* Zone, which is also defined in the area from the limestone blocks and calcareous sandstone (Kobayashi, 2012a).

5. U-Pb geochronology

Sample 10VD96 was the stratigraphically lowest sampled volcanic tuff within siliciclastic rocks at the Shigeyasu quarry, where the succession is overturned. Eight grains selected for CA-IDTIMS yielded dates ranging from 267.65 to 267.01 Ma; five of these analyses are concordant and equivalent with a weighted mean $^{206}Pb/^{238}U$ date of 267.46 ± 0.04 (0.14) [0.31] Ma (2s; MSWD = 1.90), which is interpreted as estimating the volcanic depositional age (Table 2, Fig. 6). Two analyses yielded resolvably older dates with a modified Thompson tau test, and are interpreted as representing inheritance, and a single analysis with an anomalously younger age is interpreted as the sole crystal in this study in which Pb-loss was not completely mitigated by chemical abrasion.

Sample 10VD95 from fifteen meters stratigraphically higher in the section was dated using ten single zircon grains; the five youngest analyses yielded a weighted mean $^{206}Pb/^{238}U$ date of 266.00 ± 0.04 (0.14) [0.31] Ma (2s; MSWD = 1.06), which is interpreted as estimating the volcanic depositional age (Table 2, Fig. 6). Another five grains produced older ages ranging from 266.25 to 269.85 Ma, and are attributed to inheritance.

Sample 10VD26 collected from a volcanic tuff 3.3 meters stratigraphically above sample 10VD95, and 1.7 meters below the base of the laminated limestone turbidite beds. All ten single zircons analyzed by CA-IDTIMS yielded concordant and equivalent isotope ratios within their errors, with a weighted mean $^{206}Pb/^{238}U$ date of 265.81 ± 0.04 (0.13) [0.31] Ma (2s; MSWD = 1.05), which is interpreted as the volcanic depositional age (Table 2, Fig. 6).

Samples 10VD25 and **10VD20** from the base and top of the laminated limestone turbidite bar in the Tsunemori Formation yielded indistinguishable radioisotopic ages. Ten single zircons from sample 10VD25 produced concordant and equivalent isotope ratios with a weighted mean $^{206}Pb/^{238}U$ date of 265.77 ± ± 0.03 (0.13) [0.31] Ma (2s; MSWD = 0.39), and four of seven single grains from sample 10VD20 produced a weighted mean $^{206}Pb/^{238}U$ date of 265.76 ± 0.04(0.14)[0.31] Ma (2s; MSWD = 1.60) (Table 2, Fig. 6). These dates demonstrate the expected increase in rock accumulation rate through the laminated limestone beds as compared to the underlying siliciclastic succession and affirm the effectively conformable nature of the siliciclastic-carbonate transition. The sequence of CA-IDTIMS radioisotopic ages also affirm the overturned orientation of the succession (Figs. 2-3), which is a common feature within the Tsunemori Formation (Wakita et al., 2018).

6. Discussion

6.1 Radioisotopic ages and sedimentation processes in the Tsunemori Formation.

The Tsunemori Formation at the Shigeyasu Quarry possesses all of the features of a locally normal sedimentary succession. Besides its overturned position in the quarry, it is generally stratified throughout. The laterally traceable volcanic tuffs that were found in the

Shigeyasu Quarry are marker beds of stratigraphic integrity, and could be preserved only in relatively low energy environments. The presence of two volcanic tuff horizons of the same age (10VD20 and 10VD25) within the turbiditic limestone suggests normal sedimentation therein (Wakita et al., 2018), rather than olistrosomal incorporation in a mélange environment (Sano and Kanmera, 1991b). The regular succession of radioisotopic ages from 267.46 ± 0.04 at the bottom of the exposed part of the Tsunemori Formation (samples 10VD96) to 265.76 ± 0.04 Ma at the exposed top of the formation (Figs. 2-3), combined with the consistent age of all fusulinids collected from limestone provide the most compelling evidence for conformable sedimentation within the Tsunemori Formation at the Shigeyasu Quarry.

6.2 Midian Stage of the Tethyan provincial time scale

The Midian Stage possesses a complicated history of establishment. Being proposed as a stage equal to the *Yabeina-Lepidolina* fusulinid Genozone that is well known from Japan (Toriyama, 1967), it was first referred to as the “Capitanian” Stage in the Tethys (Leven, 1975). However the Genozone and “Capitanian” Stage designation followed from compilation of the literature in Eastern Tethys without specific characterization of the stage boundaries (Leven, 1975). Furthermore strong provincialism and the lack of verbeekinids in the Capitanian of the type area in Texas (Dunbar and Skinner, 1937) has caused difficulty in fusulinid correlation of the Capitanian Stage of Texas outside of this region. Because of doubts on the exact correspondence of the *Yabeina-Lepidolina* fusulinids Genozone of the Tethys with the Capitanian Stage of Texas (Leven, 1980), a new Midian Stage equal to the Genozone was established with the potential type section in Transcaucasia. The base of the Midian Stage was first drawn at the base of the Arpa Formation in Transcaucasia without specific type sections

(Leven, 1980). The stratotype of the Stage was later proposed and the boundary defined at the base of Bed 33 in the Dzhagadzur section, Armenia, which coincided with the bottom of the Arpa Formation and with the base of the *Yangchienia thompsoni* local fusulinid Zone (Kotlyar et al., 1989). The Midian Stage in Transcaucasia is composed of massive limestone of the Arpa and Khachik Formations, totaling 350-450 m in thickness. Both the base of the Arpa and the top of Khachik Formations possess transitional contacts with the limestones below and above the Midian Stage (Kotlyar et al., 1989). The Midian Stage in Transcaucasia comprises three fusulinid zones. The Arpa Formation is divided into the *Yangchienia thompsoni* (lower) and *Chusenella abichi* (upper) Zones (Kotlyar et al., 1989). Small fusulinids *Reichelina*, *Dunbarula*, *Codonofusiella*, *Minojapanella (Wutuella)*, *Kahlerina* and *Pseudokahlerina* appear from the beginning of the Arpa Formation. No specific zone is proposed for the Khachik Formation, but in accordance with the fusulinid biota in the formation (Kotlyar et al., 1989) it could be named as the *Pseudofusulina solita -Neoschwagerina pinguis* Zone. The latter two species have been described from Turkey in associated with typical upper Midian fusulinids *Yabeina opima* and small fusulinids such as *Reichelina*, *Dunbarula*, *Codonofusiella*, *Rauserella* and *Kahlerina* (Skinner, 1969; Kotlyar et al., 1989). The Khachik Formation in Transcaucasia is conformably overlain by the Chanakhchi beds of Wuchiapingian age (Sahakyan et al., 2017).

The most confusing aspect in the designation of the Midian Stage is that no *Yabeina* or *Lepidolina* that originally were used for the concept of the stage designation (Leven, 1975) occur in the type area in Transcaucasia. Rare *Neoschwagerina cheni* Sheng, 1956, *Verbeekina verbeeki* (Geinitz) and *V. furnishi* Skinner and Wilde are found in the underlying Gnishik Formation. A single specimen of *Neoschwagerina pinguis* Skinner has been found in bed 13 of the Khachik Formation at the type section of the Midian Stage, 122 meters above the base of the Stage (Kotlyar et al., 1989). Similarly, a narrow bed with *Sumatrina vediensis* (Leven) has been reported approximately 70 meters above the base of the Arpa Formation in the Vedi section (Leven, 1998). Although the type-section of the Midian Stage is lacking the indices *Yabeina* and *Lepidolina*, it is reasonably well correlated with sections in the East Tethys thanks to its stratigraphic position below the well-defined Wuchiapingian Stage of the IGTS (Kozur, 2005) in Transcaucasia, and to the abundant assemblage of small fusulinids ozawainellids and schubertellids, such as *Kahlerina*, *Pseudokahlerina*, *Dunbarula*, *Reichelina*, *Rauserella* and numerous species of advanced schwagerinids *Chusenella* that occur within the entire Midian Stage (Kotlyar et al., 1989; Leven, 1998). These genera and the species of the latter genus are very characteristic for the Midian deposits in Peri-Gondwana (Leven, 1998; Huang et al., 2009; Leven, 2009; Davydov and Arefifard, 2013), and Cathaysian blocks including South China (Sheng, 1963; Xiao et al., 1986). However, we cannot exclude that the lowermost part of the Midian Stage corresponds with the underlying *Yabeina* and *Lepidolina* Zones in Japan and South China. The problem of precise correlation the base of the Midian Stage in Transcaucasia with the Capitanian Stage in Texas and elsewhere still exists, because of the limited characteristics of the Midian Stage in the type area, i.e. the lack of additional correlation tools, including geochemistry, paleomagnetism, and geochronology.

The Midian Stage of Japan that equates to the well-studied fusulinid *Yabeina-Lepidolina* Genozone (Toriyama, 1967), has become widely used since the Stage designation, although the position of its lower boundary in Japan was not certain. It was proposed (Leven, 1996) to include the *Neoschwagerina margaritae* Zone of Japan into the Midian Stage because of the appearance of small fusulinids *Reichelina*, *Codonofusiella*, Kahlerina in this zone, whereas the majority of Japanese micropaleontologists follow the strict definition of the stage in the sense of First Appearance Datum (FAD) and Last Appearance Datum (LAD) of *Yabeina* and *Lepidolina* genera including *Lepidolina shiraiwensis*, *L. multiseptata* and *L. kumaensis* Zones (Ozawa, 1975; Kobayashi, 2012a,b) and *Yabeina globosa* Zone in the Jurassic terrane of Japan (Kobayashi, 2011). Some Japanese paleontologists follow the suggestion of Leven (1996) and include the underlying *Yabeina-Lepidolina* Genozone, and the *Colania douvillei* Zone in the Akiyoshi Limestone into the Midian Stage (Nakazawa and Ueno, 2009).

6.3 Capitanian Stage in the type area in Texas

The Capitanian Stage in the traditional chronostratigraphic sense has been proposed in West Texas as an equivalent of the ammonoid *Timorites* Zone of earlier American literature (Glenister and Furnish, 1961). The lower boundary of the Capitanian Stage has conventionally been drawn at the base of the Hegler Member of the Bell Canyon Formation that is marking the base of the *Timorites* Zone. The genus *Timorites* though has also been recovered from the preceding Manzanita Member of the upper Cherry Canyon Formation (Glenister et al., 1999). The Capitanian was also equated with the fusulinids *Polydiexodina* Zone, which includes the provincial endemic genus *Polydiexodina*, advanced *Parafusulina*, and an abundant assemblage of small fusulinids such as *Rauserella*, *Reichelina*, *Parareichelina*, *Codonofusiella*, *Paradoxiella*, *Lantschichites*, and *Pseudokahlerina* (Dunbar and Skinner, 1937; Yang and Yancey, 2000; Nestell et al., 2006; Nestell and Nestell, 2006). The *Polydiexodina* Zone in the Glass Mountain of Texas is equated with the Vidrio and Altuda Formations (Dunbar and Skinner, 1937; Yang and Yancey,

2000) and with the Bell Canyon Formation (pre-Lamar Limestone) in the Guadalupe Mountains (Wilde, 1990).

The Capitanian (*sensu lato*) in this traditional sense seems to correspond with the entire Midian Stage of the Tethyan Scale (Wardlaw, 2000; Menning et al., 2006) (Fig. 7). However the base of the International Capitanian Stage (*sensu stricto*), is defined in the upper part of the Pinery Limestone Member of the Bell Canyon Formation near the top of Nipple Hill (southeastern Guadalupe Mountains), at 4.5 meters in the outcrop section on the south side of the hill and coinciding with the FAD of the conodont *Jinogondolella postserrata* (Glenister et al., 1999). This base of the International Capitanian (*sensu stricto*) therefore, occurs much higher in the Guadalupian succession of West Texas than the traditional base of the Capitanian (*sensu lato*). The Capitanian boundary is similarly shifted upwards from the base of the Vidrio Formation into the lower third of the Altuda Formation in the Glass Mountains. (Fig. 7) (Rohr et al., 2000). In the latter region this is approximately 100 meters above the traditional boundary, whereas the total thickness of the entire Guadalupian in the Glass and Del Norte Mountains is slightly over 300 meters (Wardlaw, 2000).

As the current base of the global Capitanian Stage (*s. s.*) appears within the regional Midian Stage of the Tethyan time scale (Fig. 7), the lower part of the Midian Stage in Tethys equates to the global Wordian Stage. This was quickly recognized by fusulinids workers who found a typical assemblage of small fusulinids *Reichelina*, *Codonofusiella*, Kahlerina and *Pseudokahlerina* along with advanced *Neoschwagerina* and some *Yabeina* in the re-defined upper Wordian Stage (Davydov, 1994; Stevens et al., 1997; Leven, 2001). Nonetheless, most Japanese and Chinese fusulinid workers still consider the Midian Stage in eastern Tethys in the traditional sense, i.e. Capitanian (*s. l.*) (Ozawa and Kobayashi, 1990; Kobayashi, 2012a,b; Kofukuda et al., 2014; Zhang and Wang, 2018). Ammonoid workers also consider the Capitanian Stage in the traditional sense as the equivalent of the *Timorites* ammonoid Genozone, because there is no opportunity to separate upper Wordian and lower Capitanian parts of the Genozone (Bogoslovskaya et al., 1995; Ehiro and Misaki, 2005; Leonova, 2018).

6.4 Biotic and radioisotopic correlation of the Midian and Capitanian Stages.

Correlation of Midian Stage of the Tethyan time scale with the IGTS has been difficult and controversial. Since its definition (Leven, 1980) , and through the mid-1990s the Midian Stage was correlated utilizing fusulinids and ammonoids with the Capitanian Stage (*s. l.*) of Texas (Jin et al., 1997). Once the Capitanian was redefined and its lower boundary in Texas shifted upwards (Glenister et al., 1999), the fusulinid assemblages from the lower Capitanian (*s.l.*) now characterize the upper Wordian of the IGTS (Davydov, 1994; Kozur and Davydov, 1996; Stevens et al., 1997).

Nevertheless, in some regions this part of the succession has remained equated with the Capitanian (Menning et al., 2006; Nakazawa and Ueno, 2009; Kobayashi, 2011, 2012a,b; Kofukuda et al., 2014). In Japan, the Guadalupian Series is divided into a several fusulinid zones (Fig. 7). The lower Midian Stage in the Akiyoshi area in our opinion correlates with the upper part of *Colania douvelei-Neoschwagerina haydeni* Zone, where the first *Kahlerina* appear (Nakazawa and Ueno, 2009; Kobayashi, 2012a,b). We suggest naming this part of the *Colania douvelei-Neoschwagerina haydeni* Zone as the *Kahlerina* beds. Following upwards, the *Lepidolina shiraiwensis* Zone together with the *Kahlerina* Beds thus correlates with the upper Wordian of the IGTS (Fig. 7). The radioisotopic ages from the Manzanita bed of Texas (Bowring et al., 1998; Ramezani and Bowring, 2018) and from the *Lepidolina shiraiwensis* Zone of Akiyoshi (this study) support such a correlation. This contrasts with and requires revision of the recent assignment of an uppermost Capitanian age for the *Lepidolina shiraiwensis* Zone in some recent publications (Zhang and Wang, 2018).

The *Kahlerina* Beds and *Lepidolina shiraiwensis* Zone of Akiyoshi and *Yabeina globosa* Zone of Akasaka consequently correlate with the Arpa Formation (lower Midian) of Transcaucasia (Kotlyar et al., 1988; Kobayashi, 2011), the lower Karasin Beds of the southeast Pamir (Chediya et al., 1986), and the *Yabeina inoyei* fusulinid Zone of South China (Mei et al., 1998). The Capitanian Stage (*s. s*.) of the IGTS correlates with the *Lepidolina multiseptata* and *L. kumaensis* Zones of Japan, the upper Midian Stage of the Tethyan time scale, the Khachik Formation of Transcaucasia, the upper Karasin Beds in the Pamirs where *Lepidolina* ex gr. *multiseptata* and *Yabeina opima* are found (Chediya et al., 1986; Kotlyar et al., 1989), and the *Metadoliolina multivoluta-Lepidolina multiseptata* fusulinid Zone of South China (Fig. 7).

7. Conclusions

The sequence of radioisotopic ages and consistent age of all fusulinids suggest a conformable sedimentary succession within the Tsunemori Formation at the Shigeyasu Quarry. The obtained radioisotopic, sedimentologic and biostratigraphic data of the Tsunemori Formation at the Shigeyasu Quarry and the presence of acidic volcanic tuffs are consistent with a forearc basin or trench slope basin as the site of deposition for the Tsunemori Formation.

The mixed volcano-siliciclastic-carbonate succession in the Tsunemori Formation at Shigeyasu Quarry, Japan, contains both fusulinids and tuffs with U-Pb zircon CA-IDTIMS radioisotopic ages that allow a robust correlation of the *Kahlerina* Beds and *Lepidolina* *shiraiwensis* Zones of Japan to the lower Midian Stage of the Tethyan time scale, and to the upper Wordian Stage of the International Geologic Time Scale.

Acknowledgements

We would like to express our gratitude to Pacific Cement Limited Company and Mr. Takano Masinori from the company for permission to access the quarry. Prof. H. Sano provided many valuable suggestions and comments in the field and in the early version of the manuscript. Reviewers Seth Burgess and Fumio Kobayashi provided valuable notes and comments that improved the manuscript. This paper was completed with support from NSF grants EAR- 1124488 (to DVI and SMD). The work was supported by the Ministry of Education and Science of the Russian Federation contract No. 14.Y26.31.0029 in the framework of the Resolution No.220 of the Government of the Russian Federation. The funds from the subsidy allocated to Kazan Federal University for the state assignment #5.2192.2017/4.6 in the sphere of scientific activities and in part from the subsidy of the Russian Government to support the Program of Competitive Growth of Kazan Federal University among the World Leading Academic Centers (to DVI) are highly appreciated.

References

Angiolini, L., Zanchi, A., Zanchetta, S., Nicora, A., Vuolo, I., Berra, F., Henderson, C., Malaspina, N., Rettori, R., Vachard, D., Vezzoli, G., 2015. From rift to drift in South Pamir (Tajikistan): Permian evolution of a Cimmerian terrane. Journal of Asian Earth Sciences 102, 146–169.

Bogoslovskaya, M.F., Leonova, T.B., Shkolin, A.A., 1995. The Carboniferous-Permian boundary and ammonoids from the Aidaralash section, southern Urals. Journal of Paleontology 69, 288–301.

Bowring, S.A., Erwin, D.H., Jin, Y.G., Martin, M.W., Davidek, K., Wang, W., 1998. U/Pb zircon geochronology and tempo of the end-Permian mass extinction. Science 280, 1039–1045.

Chediya, I.O., Bogoslovskaya, M.F., Davydov, V.I., Dmitriyev, V.Y., 1986. Fuzulinidy i ammonoidey v stratotipe kubergandinskogo yarusa (Yugo-Vostochnyy Pamir). Fusulinids and ammonoids in the stratotype of the Kubergandy Stage; southeastern Pamirs. Ezhegodnik Vsesoyuznogo Paleontologicheskogo Obshchestva 29, (In Russian) 28–53.

Cohen, K.M., Finney, S.C., Gibbard, P.L., Fan, J.X., 2013. The ICS International Chronostratigraphic Chart. Episodes 36, 199–204.

Davydov, V.I., 1994. Murgabian-Midian fusulinid zonation and the problem of correlatingthe Murgabian/Midian boundary in a global scale. Abstracts with program International Symposium on Permian Stratigraphy, Environments & Resources with International Meetings of Pangea Project GSSP, IGSP 306 & 359, 5–6.

Davydov, V.I., Arefifard, S., 2013. Middle Permian (Guadalupian) fusulinid taxonomy and biostratigraphy of the mid-latitude Dalan Basin, Zagros, Iran and their applications in paleoclimate dynamics and paleogeography. Geoarabia 18 (2), 17–62.

Davydov, V.I., Biakov, A.S., Isbell, J.L., Crowley, J.L., Schmitz, M.D., Vedernikov, I.L., 2016. Middle Permian U–Pb zircon ages of the “glacial” deposits of the Atkan Formation, Ayan-Yuryakh anticlinorium, Magadan province, NE Russia: Their significance for global climatic interpretations. Gondwana Research 38, 74–85.

Davydov, V.I., Biakov, A.S., Schmitz, M.D., Silantiev, V.V., 2018. Radioisotopic calibration of the Guadalupian (middle Permian) series: Review and updates. Earth-Science Reviews 176, 222–240.

Dunbar, C.O., Skinner, J.W., 1937. Permian Fusulinidae of Texas. The University of Texas Bulletin 3701, 517–825.

Ehiro, M., Misaki, A., 2005. Middle Permian ammonoids from the Kamiyasse-Imo district in the Southern Kitakami Massif, Northeast Japan. Paleontological Research 9 (1), 1–14.

Glenister, B.F., Furnish, W.M., 1961. The Permian ammonoids of Australia. Journal of Paleontology 35 (4), 673–736.

Glenister, B.F., Wardlaw, B.R., Lambert, L.L., Spinosa, C., Bowring, S.A., Erwin, D.H., Menning, M., Wilde, G.L., 1999. Proposal of Guadalupian and Component Roadian, Wordian and Capitanian Stages as International Standards for the Middle Permian Series. Permophiles 34, 3–11.

Gradstein, F.M., Ogg, J.G., Schmitz, M.D., Ogg, G. (Eds.), 2012. *The Geologic Time Scale 2012.* Elsevier, Amsterdam, 1176 p.

Hara, H., Hirano, M., Kurihara, T., Takahashi, T., Ueda, H., 2018. Permian arc evolution associated with Panthalassa subduction along the eastern margin of the South China block, based on sandstone provenance and U–Pb detrital zircon ages of the Kurosegawa belt, Southwest Japan. Journal of Asian Earth Sciences 151, 112–130.

Henderson, C., Davydov, V.I., Wardlaw, B.R., 2012. The Permian Period, in: Gradstein, F.M., Ogg, J.G., Schmitz, M.D., Ogg, G. (Eds.), The Geologic Time Scale 2012, vol. 2. Elsevier, Amsterdam, pp. 653–679.

Huang, H., Jin, X., Shi, Y., Yang, X., 2009. Middle Permian western Tethyan fusulinids from southern Baoshan Block, western Yunnan, China. J. Paleontol. 83 (06), 880–896.

Jin, Y., Wardlaw, B.R., Gleinster, B.F., Kotlyar, G.V., 1997. Permian chronostratigraphic subdivisions. Episodes 20 (1), 10–15.

Kanmera, K., 1974. Paleozoic and Mesozoic geosynclinal volcanism in the Japanese Islands and associated chert sedimentation. Special Publication - Society of Economic Paleontologists and Mineralogists 19, 161–173.

Kanmera, K., Nishi, H., 1983. Accreted ocean reef complex in southwest Japan. In: Hashimoto, M., Ueda, S. (Eds.), Accretion Tectonics in the Circum-Pacific regions. Terra Scientific Publishing Company, Tokyo.

Kobayashi, F., 2011. Permian fusuline faunas and biostratigraphy of the Akasaka Limestone (Japan). Revue de Paléobiologie 30 (2), 431–574.

Kobayashi, F., 2012a. Late Paleozoic foraminifers from limestone blocks and fragments of the Permian Tsunemori Formation and their connection to the Akiyoshi Limestone Group, Southwest Japan. Paleontological Research 16 (3), 219–243.

Kobayashi, F., 2012b. Comparative study of the Capitanian (late Guadalupian) foraminiferal faunas in the *Lepidolina shiraiwensis* Zone of the Akiyoshi limestone group, SW Japan. The Journal of Foraminiferal Research 42 (1), 82–101.

Kofukuda, D., Isozaki, Y., Igo, H., 2014. A remarkable sea-level drop and relevant biotic responses across the Guadalupian–Lopingian (Permian) boundary in low-latitude mid-Panthalassa: Irreversible changes recorded in accreted paleo-atoll limestones in Akasaka and Ishiyama, Japan. Journal of Asian Earth Sciences 82, 47–65.

Kotlyar, G.V., Chediya, I.O., Kropacheva, G.S., Pronina, G.P., Rostovtsev, K.O., 1988. Regional biostratigraphic scales and sections of the Transcaucasian Permian deposits. Sovetskaya Geologiya (2), (In Russian) 47–57.

Kotlyar, G.V., Zakharov, Y.D., Kropacheva, G.S., Pronina, G.P., Chedija, I.O., Burago, V.I., 1989. Evolution of the latest Permian Biota. Midian regional stages in the USSR. Nauka, Leningrad (In Russian).

Kozur, H., 2005. Pelagic uppermost Permian and the Permian-Triassic boundary conodonts of Iran. Part 2. Investigated sections and evaluation of the conodont faunas. Hallesches Jahrb. Geowiss., B Beiheft 19, 49–86.

Kozur, H., Davydov, V.I., 1996. The importance of the Permian of the Sosio Valley (Western Sicily, Italy) for Guadalupian Stratigraphy. Abstracts and proceedings of the Second International Guadalupian Symposium, 11–15.

Kozur, H., Davydov, V.I., Kotlyar, G.V., 1994. Preliminary report on the Permian conodont fauna of Darvas and SE Pamir and its importance for the Permian time scale and its importance for the Permian Time Scale. Permophiles (24), 13–15.

Leonova, T.B., 2018. Permian ammonoid biostratigraphy, in: Lucas, S.G., Shen, S. (Eds.), The Permian Times. Special Publications, pp. 185–203.

Leven, E.J., 1980. Explonatory notes to the Stratigraphic Scale of the Permian deposits of Tethyan Realm. Leningrad, VSEGEI Institute, (In Russian) 1-51.

Leven, E.J., 1998. Permian fusulinid assemblages and stratigraphy of the Transcaucasia. Rivista Italiana di Paleontologia e Stratigrafia 104 (3), 299–328.

Leven, E.J., 2001. On possibility of using the global Permian Stage scale in the Tethyan region. Stratigraphy and Geological Correlation 9 (2), 118-131.

Leven, E.J., 2009. The Upper Carboniferous (Pennsylvanian) and Permian of the Western Tethys: fusulinids, stratigraphy, biogeography. GEOS, Moscow, 246 (In Russian).

Leven, E.Y., 1967. Stratigrafiya i fuzulinidy permskikh otlozheniy Pamira; stratigraphy and fusulinides of the Pamirs Permian deposits. Trudy - Geologicheskiy Institut (Moskva) 167, 215 (In Russian).

Leven, E.Y., 1975. Yarusnaya shkala permskikh otlozheniy Tetisa. The stage scale of the Permian deposits of the Tethys. Byulleten' Moskovskogo Obshchestva Ispytateley Prirody, Otdel Geologicheskiy 50 (1), (In Russian) 5–21.

Leven, E.Y., 1996. Midiyskiy yarus permi i yego granitsy. Permian Midian stage and its boundaries. Stratigrafiya, Geologicheskaya Korrelyatsiya 4 (6), (In Russian) 20–31.

Mattinson, J.M., 2005. Zircon U-Pb chemical abrasion ("CA-TIMS") method: combined annealing and multi-step partial dissolution analysis for improved precision and accuracy of zircon ages. Chemical Geology 220, 47–66.

Mei, S., Jin, Y.G., Wardlaw, B.R., 1998. Conodont succession of the Guadalupian-Lopingian boundary strata in Laibin of Guangxi, China and West Texas, USA. Palaeoworld (9).

Menning, M., Alekseev, A.S., Chuvashov, B.I., Davydov, V.I., Devuyst, F.X., Forke, H.C., Grunt, T.A., Hance, L., Heckel, P.H., Izokh, N.G., Jin, Y.G., Jones, P.J., Kotlyar, G.V., Kozur, H.W., Nemyrovska, T.I., Schneider, J.W., Wang, X.D., Weddige, K., Weyer, D., Work, D.M., 2006. Global time scale and regional stratigraphic reference scales of central and west Europe, east Europe, Tethys, south China, and North America as used in the Devonian-

Carboniferous-Permian Correlation Chart 2003 (DCP 2003). Palaeogeography, Palaeoclimatology, Palaeoecology 240 (1-2), 318–372.

Nakazawa, T., Ueno, K., 2009. Carboniferous-Permian long-term sea-level change inferred from Panthalassan oceanic atoll stratigraphy. Palaeoworld 18 (2-3), 162–168.

Nestell, G.P., Nestell, M.K., 2006. Middle Permian (Late Guadalupian) foraminifers from Dark Canyon, Guadalupe Mountains, New Mexico. Micropaleontology 52 (1), 1–50.

Nestell, M.K., Nestell, G.P., Wardlaw, B.R., Sweatt, M.J., 2006. Integrated biostratigraphy of foraminifers, radiolarians and conodonts in shallow and deep water Middle Permian (Capitanian) deposits of the “Rader slide”, Guadalupe Mountains,West Texas. Stratigraphy 3 (3), 161–194.

Okawa, H., Shimojo, M., Orinashi, Y., Yamamoto, K., Hirata, T., Sano, S.-i., Isozaki, Y., Kouchi, Y., Yanai, S., Otoh, S., h, 2013. Detrital zircon geochronology of the Silurian–lower Cretaceous continuous succession of the South Kitakami belt, Northeast Japan. Memoir of the Fukui Prefectural Dinosaur Museum 12, 35–78.

Ozawa, T., 1975. Evolution of Lepidolina multiseptata; Permian foraminifer, in East Asia. Memoirs of the Faculty of Science, Kyushu University, Series D: Geology 23 (2), 117–164.

Ozawa, T., Kobayashi, F., 1990. Carboniferous to Permian Akiyoshi Limestone Group: Ozawa, T. & F. Kobayashi (1990) - Carboniferous to Permian Akiyoshi Limestone Group. In : Organization Committee Benthos ‘90 (ed.), Fossils and recent benthic foraminifera in some selected regions in Japan. Guidebook for field trips, 4th International Symposium on Benthic Foraminifera, Sendai, 1990, E1-E31. In : Organization Committee Benthos ‘90 (ed.), Fossils and recent benthic foraminifera in some selected regions in Japan. Guidebook for field trips, 4th International Symposium on Benthic Foraminifera, E1-E31.

Ozawa, T., Kobayashi, F., Watanabe, K., 1991. Biostratigraphic zonation of Late Carboniferous to Early Permian sequence of the Akiyoshi Limestone Group, Japan and its correlation with reference sections in the Tethyan region. Proceedings of the International Symposium on Shallow Tethys 3, 327–341.

Ramezani, J., Bowring, S.A., 2018. Advances in numerical calibration of the Permian timescale based on radioisotopic geochronology, in: Lucas, S.G., Shen, S. (Eds.), *The Permian Timescale*. Special Publication - Geological Society of London 480, 51–60.

Rohr, D., Wardlaw, B.R., Rudine, S.F., Hafeef, M., Hall, A.J., Grant, R.E., 2000. Guidebook to the Guadalupian Symposium., in: Wardlaw, B.R., Grant, R.E., Rohr, D.M. (Eds.), The Guadalupian Symposium. Smithsonian Contribution to the Earth Sciences, No 32, vol. 32. Smithsonian Institute Press, Washington, DC, pp. 5–36.

Sahakyan, L., Baud, A., Grigoryan, A., Friesenbichler, E., Richoz, S. (Eds.), 2017. The Permian-Triassic transition in southern Armenia. IGCP 630 Field Workshop in Armenia. Institute of Geological Sciences, National Academy of Sciences of Armenia, Yerevan, 54 pp.

Sano, H., Kanmera, K., 1991a. Collapse of ancient oceanic reef complex; what happened during collision of Akiyoshi reef?: Limestone breccias, redeposited limestone debris and mudstone injections. Chishitsugaku Zasshi = Journal of the Geological Society of Japan 97 (4), 297–309.

Sano, H., Kanmera, K., 1991b. Collapse of ancient oceanic reef complex; what happened during collision of Akiyoshi reef?: Limestone breccias, redeposited limestone debris and mudstone injections. Chishitsugaku Zasshi = Journal of the Geological Society of Japan 97 (4), 297–309.

Sano, H., Kanmera, K., 1991c. Collapse of ancient oceanic reef complex; what happened during collision of Akiyoshi reef?: Sequence of collisional collapse and generation of collapse products. Chishitsugaku Zasshi = Journal of the Geological Society of Japan 97 (8), 631–644.

Sheng, J.-Z., 1963. Permian fusulinids of Kwangsi, Kueichow and Szechuan.: Palaeontologica Sinica, vol. 149, New Series B, No 10, 111-247. Schience Press, Peking.

Skinner, J.W., 1969. Permian foraminifera from Turkey. University of Kansas Paleontological Contributions, Paper 36, 14 p.

Stevens, C.H., Davydov, V.I., Bradley, D.C., 1997. Permian Tethyan Fusulinina from the Kenai Peninsula, Alaska. Journal of Paleontology 71 (6), 985–994.

Tazawa, J.-i., Fujikawa, M., Ota, Y., 2009. Permian brachiopods from the Tsunemori Formation of the Akiyoshi area, southwest Japan: Fossil evidence for the accretion site of the Akiyoshi Terrane. Jour. Geol. Soc. Japan 115 (4), 168–176.

Toriyama, R., 1967. The fusulinacean zones of Japan. Memoirs of the Faculty of Science, Kyushu University, Series D, Earth and Planetary Sciences 18 (1), 35–260.

Ueno, K., 1992. Verbeekinid and Neoschwagerinid fusulinaceans from the Akiyoshi Limestone Group above the *Parafusulina kaerimizensis* Zone, Southwest Japan. Transactions and Proceedings of the Palaeontological Society of Japan. New Series 165, 1040–1069.

Wakita, K., 2013. Geology and tectonics of Japanese islands: A review – The key to understanding the geology of Asia. Journal of Asian Earth Sciences 72, 75–87.

Wakita, K., Yoshida, R., Fushimi, Y., 2018. Tectonic setting for Tsunemori Formation in the Permian accretionary complex of the Akiyoshi Belt, Southwest Japan. Heliyon 4 (12), e01084.

Wardlaw, B.R., 2000. Guadalupian Conodont Biostratigraphy of the Glass and Del Norte Mountains, in: Wardlaw, B.R., Grant, R.E., Rohr, D.M. (Eds.), The Guadalupian Symposium. Smithsonian Contribution to the Earth Sciences, No 32. Smithsonian Institute Press, Washington, DC, pp. 37–88.

Wilde, G.L., 1990. Practical fusulinid zonation: the species concept; with Permian basin emphasis. West Texas Geological Society 29, 5–34.

Wu, Q., Ramezani, J., Zhang, H., Wang, T., Yuan, D., Mu, L., Zhang, Y., Li, X., Shen, S., 2017. Calibrating the Guadalupian Series (Middle Permian) of south China. Palaeogeography, Palaeoclimatology, Palaeoecology 466, 361–372.

Xiao, W., Wang, H., Zhang, L., Dong, W.-l., 1986. Early permian stratigraphy and faunas in Southern Guizhou. The People's Publishing House of Guizhou, Guizhou, China, 1-364 (In Chinese).

Yang, Z., Yancey, T.E., 2000. Fusulinid Biostratigraphy and Paleontology of the Middle Permian (Guadalupian) Strata of the Glass Mountains and Del Norte Mountains, West Texas, in: Wardlaw, B.R., Grant, R.E., Rohr, D.M. (Eds.), The Guadalupian Symposium. Smithsonian Contribution to the Earth Sciences, No 32. Smithsonian Institute Press, Washington, DC, pp. 185–260.

Zhang, X., Takeuchi, M., Ohkawa, M., Matsuzawa, N., 2018. Provenance of a Permian accretionary complex (Nishiki Group) of the Akiyoshi Belt in Southwest Japan and Paleogeographic implications. Journal of Asian Earth Sciences.

Zhang, Y.-C., Wang, Y., 2018. Permian fusuline biostratigraphy, in: Lucas, S.G., Shen, S. (Eds.), The Permian Times. Special Publications, pp. 253–288.

Figure and Tables Captions

Figure 1. Paleogeographic and tectonic maps. (**A**) Middle Permian global paleogeography with the main regions discussed in this paper; (**B**) Regional tectonic map of southern Japan, modified from Wakita (2013).

Figure 2. **Shigeyasu Quarry**: **a**, Google Earth image of Shigeyasu Quarry, red line shows collection site; **b**, general panorama of studied site; **c**, volcanic ash (10VD20) within the laminated limestone. Stratification is well expressed within the Shigeyasu Quarry cut.

Figure 3. Stratigraphic log of the succession in Shigeyasu Quarry and position of the collected samples. Note that the succession is overturned. All scale bars of the fusulinid images are 1 mm. The entire set of the radioisotopic age attributes can be seen in Table 2.

Figure 4. Fusulinid assemblage from turbiditic bed (samples 10VD20-10VD23). 1, *Schubertella ovalis* Kobayashi; 2, *Yangchienia*? sp.; 3, *Kahlerina* sp.; 4-5, *Chusenella altinensis* Ross; 6, *Chusenella otai* (Nogami); 7-12, *Lepidolina shiraiwensis* (Ozawa); 13, *Sumatrina longissima* Deprat. All scale bars are 1 mm.

Figure 5. Fusulinid assemblage from slump block (sample 10VD98). 1, *Codonofusiella* sp.; 2, boultoniids; *Kahlerina ampla* Han; 4-7, *Kahlerina nautiloidea* Sosnina; 8, *Kahlerina* sp.; 9, *Rauserella* ex gr. *ellipsoidalis* Sosnina; 10, *Chusenella altinensis* Ross; 11, *Chusenella otai* (Nogami); 12-15, *Lepidolina shiraiwensis* (Ozawa); 16, *Sumatrina longissima* Deprat; 17, *Pseudodoliolina ozawai* Yabe and Hanzawa. All scale bars are 1mm.

Figure 6. U-Pb concordia diagrams illustrating results of single grain chemical abrasion ID-TIMS analysis for each dated tuff samples from Shigeyasu Quarry, volcano-siliciclastic succession of the Akiyoshi Plateau, southwest Japan. Grey band represents the error envelope on the concordia curve based upon the decay constants and errors of Jaffey et al. (1975). Analyses accepted in weighted mean calculations are illustrated by filled translucent ellipses; analyses discarded as influenced by inheritance or Pb-loss are illustrated as open ellipses. All accepted analyses are concordant within the decay constant uncertainties.

Figure 7. Biostratigraphic and radioisotopic correlation of the Guadalupian of Shigeyasu Quarry with major global sections: Texas (Glenister et al., 1999; Wardlaw, 2000; Yang and Yancey, 2000; Nestell et al., 2006; Nestell and Nestell, 2006); Japan (Ueno, 1992; Nakazawa and Ueno, 2009; Kobayashi, 2012a); Transcaucasia (Kotlyar et al., 1989a; Leven, 1998); Pamirs (Leven, 1967; Chediya et al., 1986; Kozur et al., 1994; Angiolini et al., 2015) and our own data; South China from (Mei et al., 1998; Wu et al., 2017).

Table 1. Fusulinid taxonomic composition of the studied limestone samples.

Table 2. Zircon IDTIMS U-Pb isotopic data

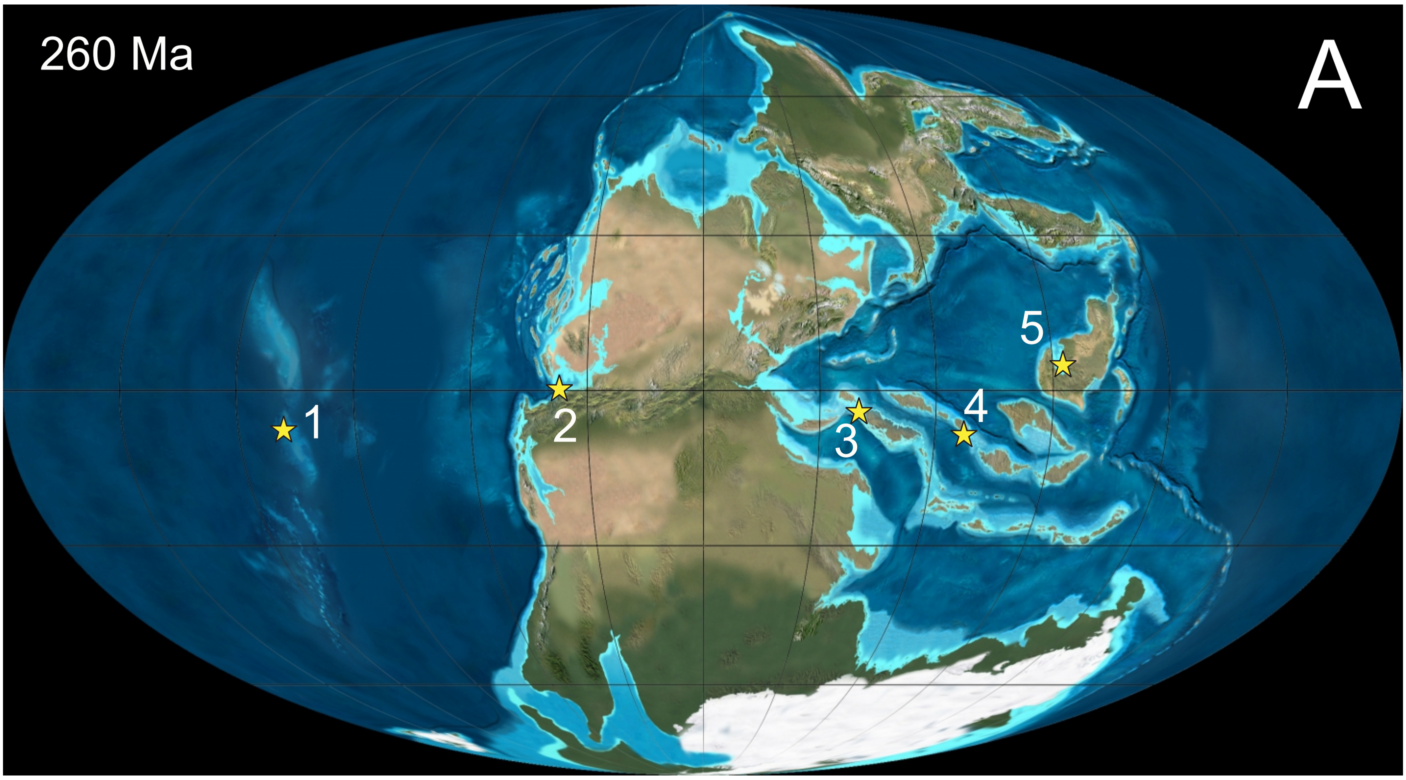

1, Akiyoshi atoll; 2, West Texas Basin; 3, Transcaucasia; 4, S-E Pamirs; 5, S. China

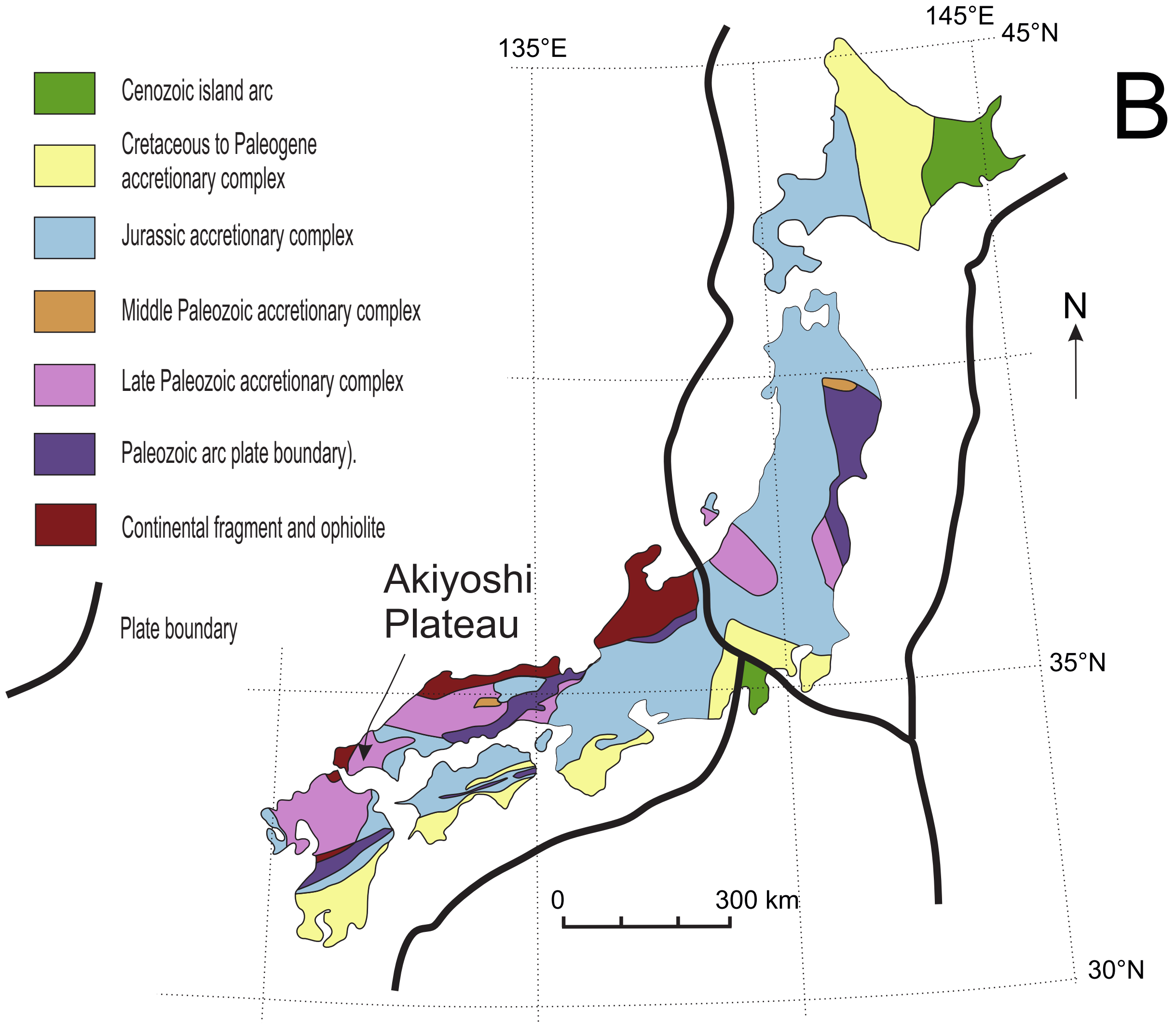

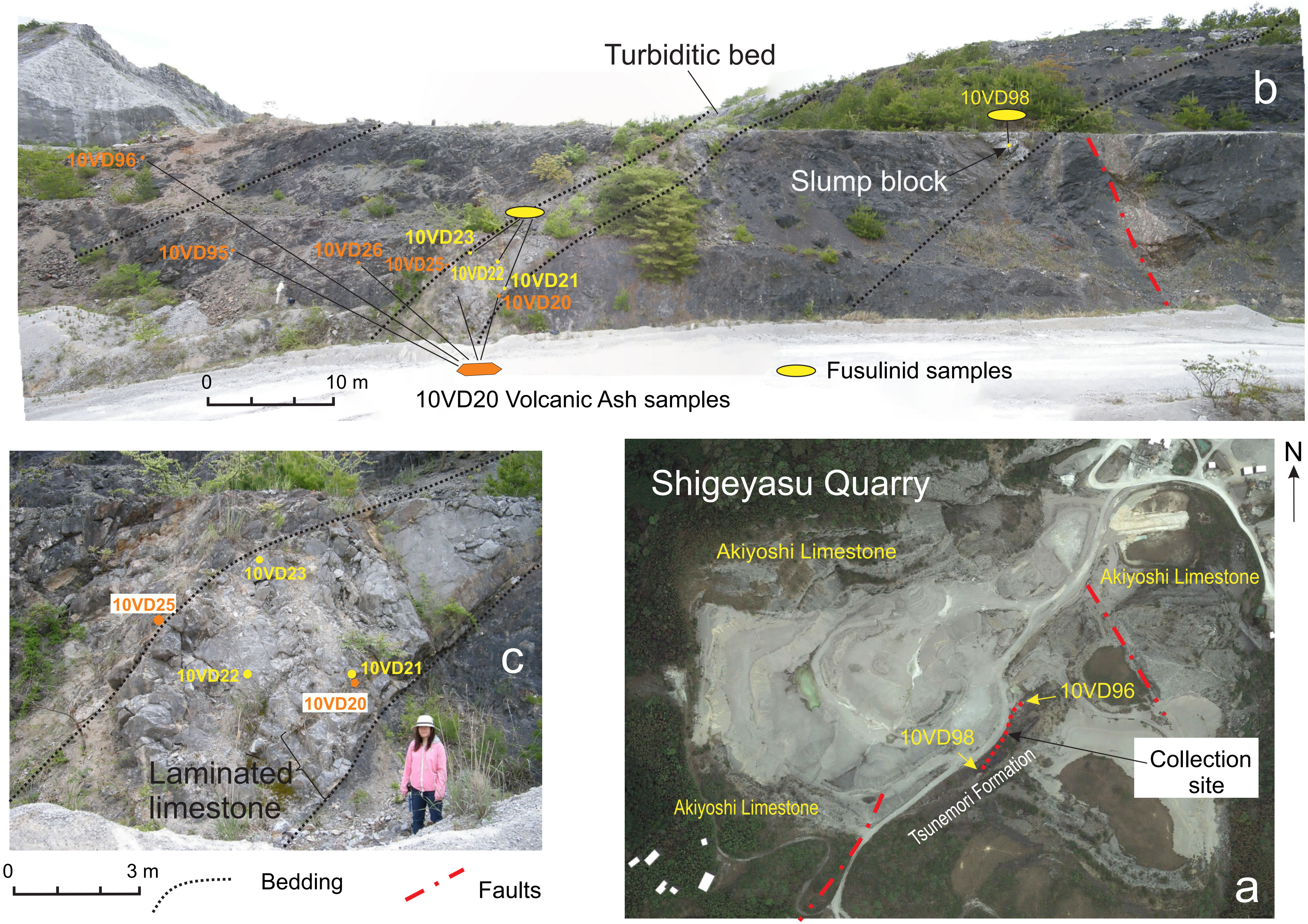

Fig. 2. Davydov and Schmitz

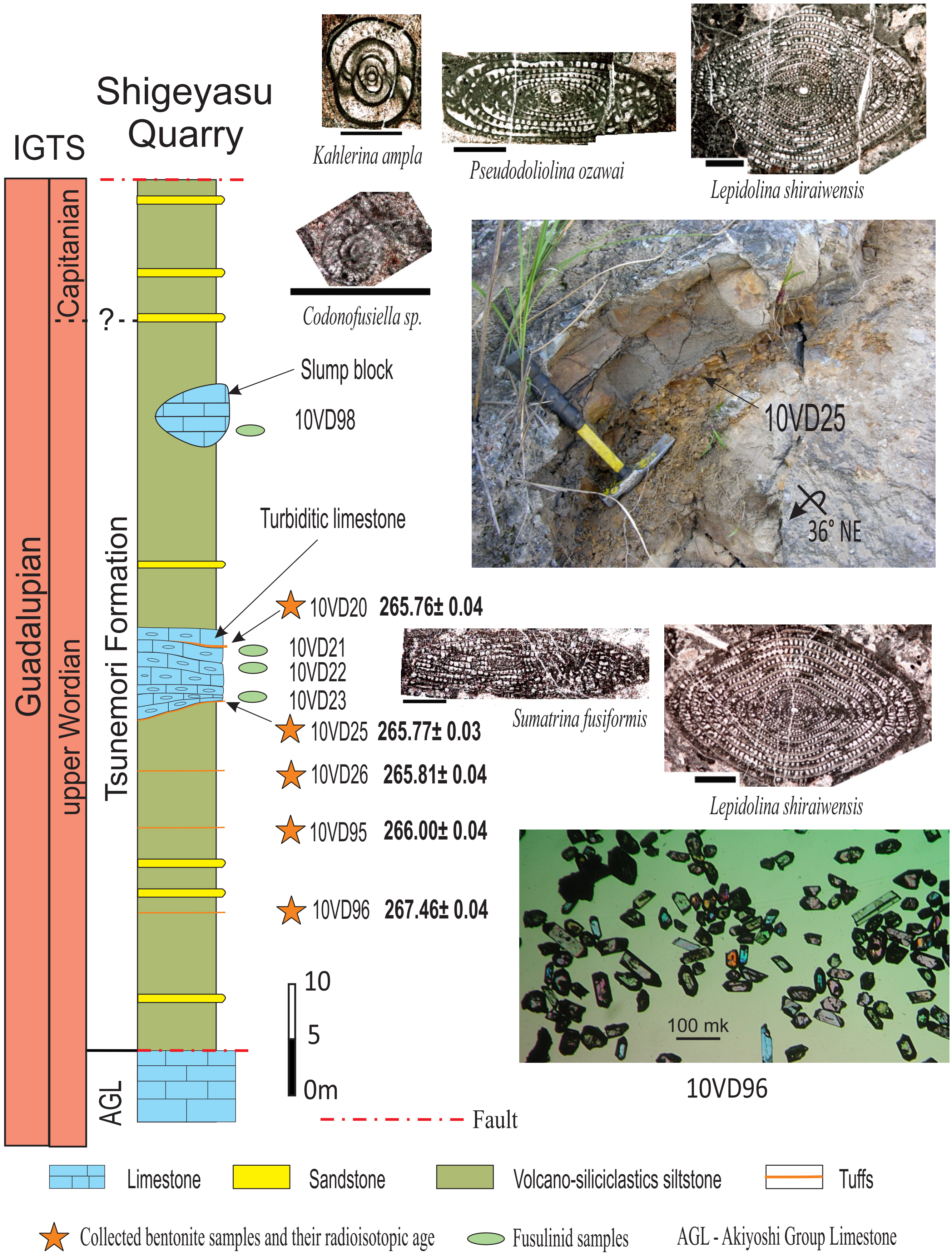

Fig. 3 Davydov and Schmitz

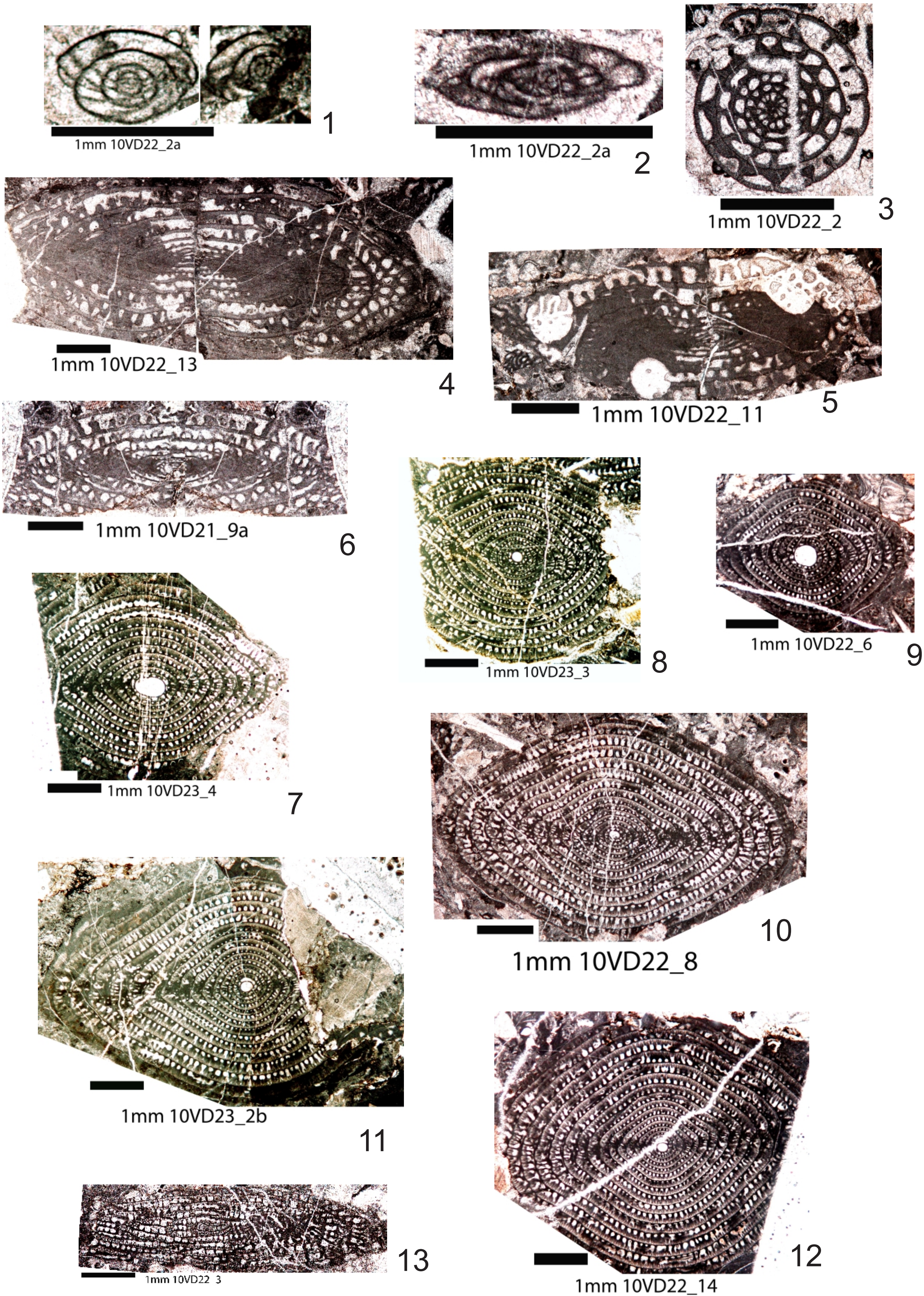

Fig. 5. Davydov and Schmitz

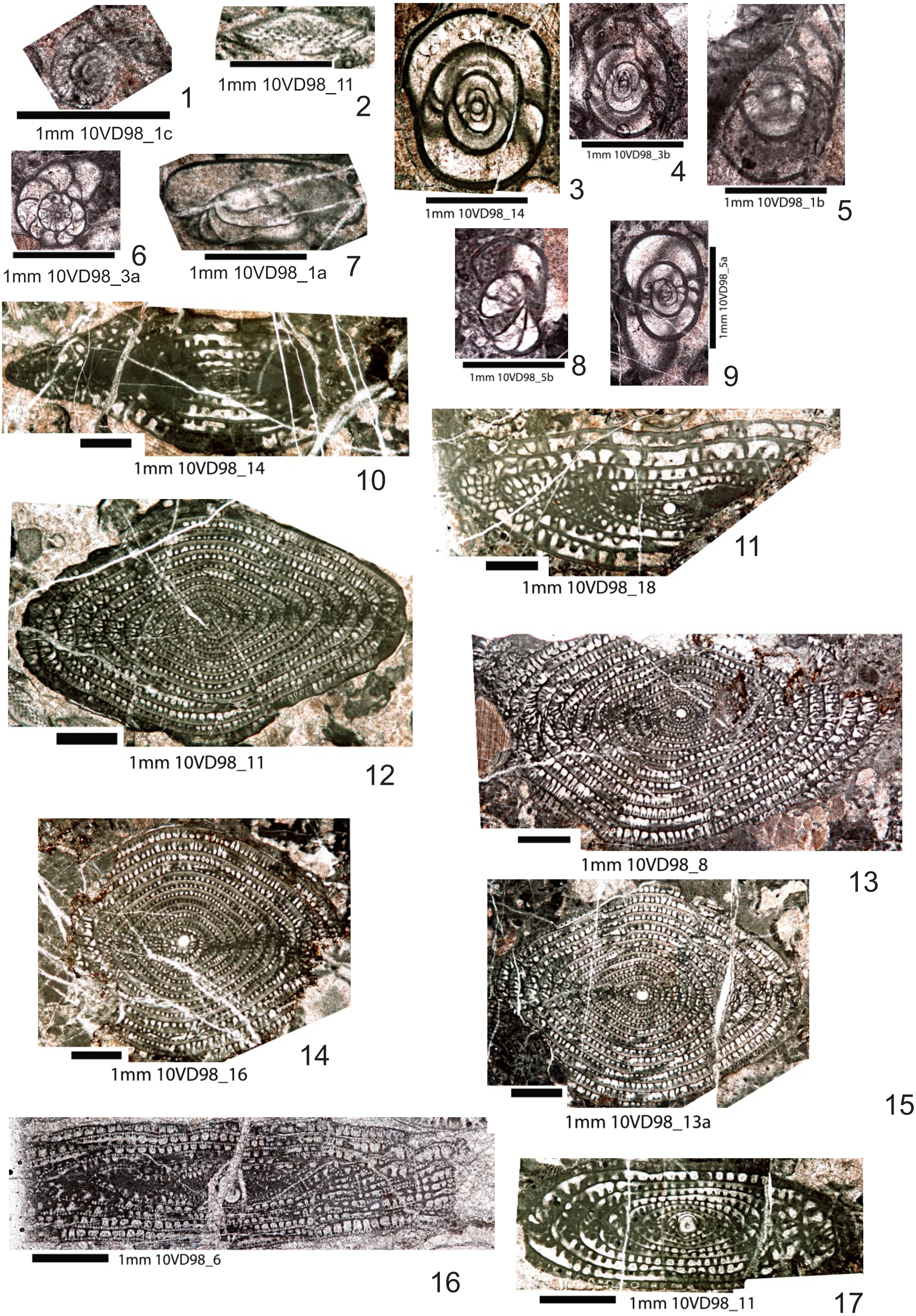

Fig. 5. Davydov and Schmitz

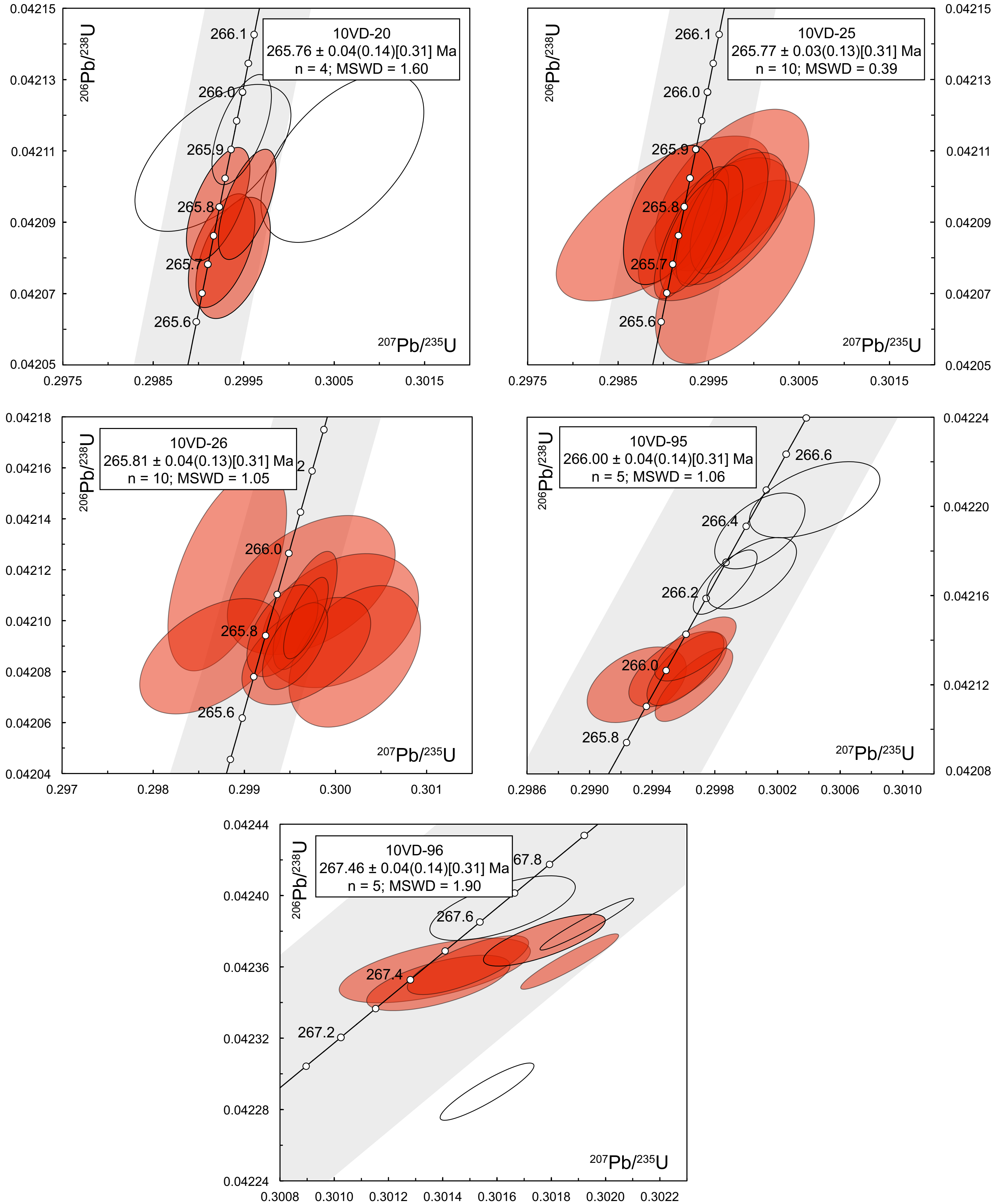

Fig. 6 Davydov and Schmitz

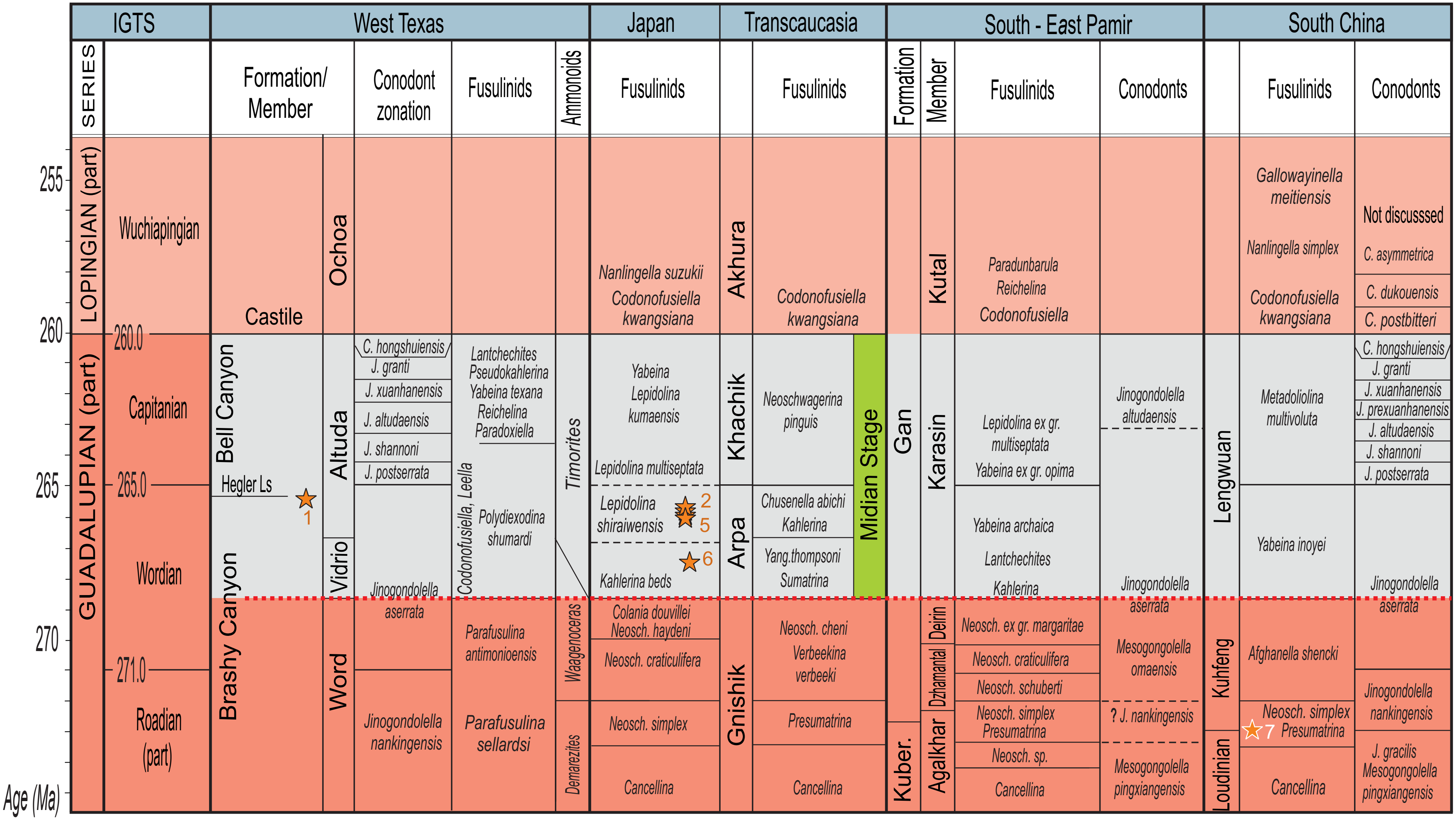

1, 265.3 ± 0.2 Ma; 2, 265.79 ± 0.04 Ma; 3, 265.77 ± 0.03 Ma; 4, 265.81 ± 0.04 Ma; 5, 266.0 ± 0.04 Ma; 6, 267.46 ± 0.04 Ma; 7, 272.95 ± 0.11 Ma

C. - Clarkina; J. - Jinogondolella; Neoschw. - Neoscwagerina; Kuber. - Kubergandy; .... Traditional base of the Capitanian Stage

Table 2. Zircon CA-IDTIMS U-Pb isotopic data

							Radiogenic Isotopic Ratios								Radiogenic Isotopic Dates					
Grain (a)	Th/U (b)	$^{206}Pb^*$ x10^{-13} mol (c)	mol % $^{206}Pb^*$ (c)	Pb^*/Pbc (c)	Pbc (pg) (c)	$^{206}Pb/^{204}Pb$ (d)	$^{208}Pb/^{206}Pb$ (e)	$^{207}Pb/^{206}Pb$ (e)	% err (f)	$^{207}Pb/^{235}U$ (e)	% err (f)	$^{206}Pb/^{238}U$ (e)	% err (f)	corr. coef.	$^{207}Pb/^{206}Pb$ (g)	± (f)	$^{207}Pb/^{235}U$ (g)	± (f)	$^{206}Pb/^{238}U$ (g)	± (f)
10VD-20																				
z1	0.747	0.9576	0.997	122	0.21	6865	0.237	0.05157	0.1	0.299481	0.1	0.042116	0.030	0.608	267	2	265.99	0.21	265.93	0.08
z7	0.572	0.3661	0.992	37	0.25	2179	0.181	0.05178	0.2	0.300602	0.2	0.042108	0.046	0.543	275	5	266.87	0.58	265.89	0.12
z6	0.504	0.6164	0.987	23	0.67	1408	0.160	0.05153	0.2	0.299162	0.2	0.042108	0.040	0.582	265	5	265.75	0.55	265.88	0.10
z5	**0.693**	**0.9609**	**0.996**	**88**	**0.29**	**5036**	**0.220**	**0.05155**	**0.1**	**0.299221**	**0.1**	**0.042095**	**0.031**	**0.626**	**266**	**2**	**265.79**	**0.22**	**265.81**	**0.08**
z4	**0.730**	**1.3211**	**0.997**	**103**	**0.34**	**5864**	**0.231**	**0.05161**	**0.1**	**0.299542**	**0.1**	**0.042095**	**0.030**	**0.631**	**268**	**2**	**266.04**	**0.20**	**265.81**	**0.08**
z2	**0.730**	**0.9618**	**0.997**	**104**	**0.24**	**5915**	**0.231**	**0.05158**	**0.1**	**0.299260**	**0.1**	**0.042082**	**0.031**	**0.515**	**267**	**2**	**265.82**	**0.24**	**265.72**	**0.08**
z3	**0.705**	**1.6631**	**0.996**	**83**	**0.53**	**4736**	**0.224**	**0.05160**	**0.1**	**0.299384**	**0.1**	**0.042080**	**0.033**	**0.462**	**268**	**2**	**265.92**	**0.26**	**265.71**	**0.09**
weighted mean $^{206}Pb/^{238}U$ age = 265.76 ± 0.04 (0.14) [0.31] Ma Ma (2s); MSWD = 1.60 (n=4)																				
10VD-25																				
z2	**0.640**	**0.5062**	**0.992**	**39**	**0.33**	**2294**	**0.203**	**0.05164**	**0.2**	**0.299762**	**0.2**	**0.042099**	**0.044**	**0.560**	**270**	**5**	**266.21**	**0.55**	**265.83**	**0.11**
z4	**0.474**	**0.6459**	**0.996**	**81**	**0.20**	**4920**	**0.150**	**0.05165**	**0.1**	**0.299733**	**0.1**	**0.042093**	**0.034**	**0.601**	**270**	**2**	**266.19**	**0.28**	**265.79**	**0.09**
z8	**0.517**	**0.6167**	**0.996**	**85**	**0.18**	**5078**	**0.164**	**0.05153**	**0.1**	**0.299061**	**0.1**	**0.042092**	**0.038**	**0.515**	**265**	**3**	**265.67**	**0.32**	**265.79**	**0.10**
z5	**0.401**	**0.4466**	**0.994**	**51**	**0.21**	**3135**	**0.127**	**0.05165**	**0.2**	**0.299724**	**0.2**	**0.042091**	**0.036**	**0.588**	**270**	**4**	**266.18**	**0.41**	**265.78**	**0.09**
z7	**0.661**	**0.2318**	**0.989**	**29**	**0.21**	**1695**	**0.209**	**0.05152**	**0.3**	**0.298998**	**0.3**	**0.042091**	**0.045**	**0.672**	**264**	**7**	**265.62**	**0.76**	**265.78**	**0.12**
z1	**0.602**	**0.8236**	**0.996**	**83**	**0.25**	**4889**	**0.191**	**0.05161**	**0.1**	**0.299514**	**0.1**	**0.042089**	**0.033**	**0.657**	**268**	**2**	**266.02**	**0.24**	**265.77**	**0.09**
z6	**0.742**	**0.4629**	**0.993**	**44**	**0.28**	**2515**	**0.235**	**0.05162**	**0.2**	**0.299568**	**0.2**	**0.042088**	**0.039**	**0.582**	**269**	**5**	**266.06**	**0.54**	**265.76**	**0.10**
z3	**0.646**	**0.7450**	**0.996**	**85**	**0.23**	**4951**	**0.205**	**0.05158**	**0.1**	**0.299313**	**0.1**	**0.042087**	**0.036**	**0.771**	**267**	**2**	**265.86**	**0.26**	**265.76**	**0.09**
z10	**0.630**	**0.7297**	**0.997**	**96**	**0.20**	**5571**	**0.200**	**0.05159**	**0.1**	**0.299338**	**0.1**	**0.042086**	**0.031**	**0.660**	**267**	**2**	**265.88**	**0.24**	**265.75**	**0.08**
z9	**0.732**	**0.3427**	**0.992**	**41**	**0.22**	**2352**	**0.232**	**0.05168**	**0.2**	**0.299797**	**0.2**	**0.042076**	**0.050**	**0.567**	**271**	**5**	**266.24**	**0.56**	**265.69**	**0.13**
weighted mean $^{206}Pb/^{238}U$ age = 265.77 ± 0.03 (0.13) [0.31] Ma Ma (2s); MSWD = 0.39 (n=10)																				
10VD-26																				
z5	**0.604**	**0.6881**	**0.996**	**80**	**0.22**	**4716**	**0.191**	**0.05145**	**0.1**	**0.298812**	**0.2**	**0.042120**	**0.077**	**0.564**	**261**	**3**	**265.47**	**0.42**	**265.96**	**0.20**
z9	**0.754**	**0.4084**	**0.992**	**39**	**0.28**	**2216**	**0.239**	**0.05162**	**0.2**	**0.299737**	**0.3**	**0.042114**	**0.053**	**0.440**	**269**	**5**	**266.19**	**0.59**	**265.92**	**0.14**
z8	**0.529**	**1.0216**	**0.997**	**117**	**0.22**	**7011**	**0.168**	**0.05162**	**0.1**	**0.299668**	**0.1**	**0.042104**	**0.045**	**0.696**	**269**	**2**	**266.14**	**0.22**	**265.86**	**0.12**
z2	**0.997**	**2.2386**	**0.998**	**170**	**0.37**	**9017**	**0.316**	**0.05163**	**0.1**	**0.299676**	**0.1**	**0.042101**	**0.031**	**0.724**	**269**	**1**	**266.15**	**0.16**	**265.84**	**0.08**
z7	**0.697**	**0.5274**	**0.995**	**64**	**0.22**	**3658**	**0.221**	**0.05169**	**0.2**	**0.300055**	**0.2**	**0.042100**	**0.051**	**0.328**	**272**	**5**	**266.44**	**0.55**	**265.84**	**0.13**
z4	**0.676**	**1.0657**	**0.998**	**126**	**0.22**	**7225**	**0.214**	**0.05159**	**0.1**	**0.299419**	**0.1**	**0.042096**	**0.035**	**0.541**	**267**	**2**	**265.95**	**0.25**	**265.81**	**0.09**
z3	**0.616**	**1.0260**	**0.997**	**106**	**0.25**	**6209**	**0.195**	**0.05162**	**0.1**	**0.299557**	**0.1**	**0.042090**	**0.033**	**0.576**	**269**	**2**	**266.05**	**0.23**	**265.78**	**0.09**
z10	**0.533**	**0.4149**	**0.994**	**50**	**0.21**	**2977**	**0.169**	**0.05164**	**0.2**	**0.299682**	**0.2**	**0.042088**	**0.041**	**0.514**	**270**	**4**	**266.15**	**0.45**	**265.76**	**0.11**
z1	**0.573**	**0.5362**	**0.994**	**53**	**0.26**	**3155**	**0.182**	**0.05174**	**0.2**	**0.300215**	**0.2**	**0.042086**	**0.054**	**0.405**	**274**	**4**	**266.57**	**0.46**	**265.75**	**0.14**
z6	**0.482**	**0.8388**	**0.988**	**24**	**0.88**	**1456**	**0.153**	**0.05146**	**0.2**	**0.298627**	**0.2**	**0.042086**	**0.044**	**0.490**	**262**	**4**	**265.33**	**0.50**	**265.75**	**0.11**
weighted mean $^{206}Pb/^{238}U$ age = 265.81 ± 0.04 (0.13) [0.31] Ma (2s); MSWD = 1.05 (n=10)																				

Table 2 continued

							Radiogenic Isotopic Ratios								Radiogenic Isotopic Dates					
Grain (a)	Th/U (b)	^{206}Pb* x10^{-13} mol (c)	mol % ^{206}Pb* (c)	Pb*/Pbc (c)	Pbc (pg) (c)	^{206}Pb/^{204}Pb (d)	^{208}Pb/^{206}Pb (e)	^{207}Pb/^{206}Pb (e)	% err (f)	^{207}Pb/^{235}U (e)	% err (f)	^{206}Pb/^{238}U (e)	% err (f)	corr. coef.	^{207}Pb/^{206}Pb (g)	± (f)	^{207}Pb/^{235}U (g)	± (f)	^{206}Pb/^{238}U (g)	± (f)
10VD-95																				
z10	0.669	0.4608	0.995	60	0.20	3468	0.212	0.05162	0.1	0.304248	0.2	0.042749	0.061	0.557	269	3	269.71	0.39	269.85	0.16
z2	0.671	1.3504	0.996	81	0.43	4678	0.213	0.05163	0.1	0.300443	0.1	0.042203	0.033	0.525	269	2	266.75	0.27	266.47	0.09
z7	0.689	1.8592	0.999	251	0.19	14366	0.218	0.05159	0.1	0.300090	0.1	0.042189	0.033	0.543	267	2	266.47	0.19	266.38	0.09
z3	0.649	1.3590	0.998	145	0.24	8360	0.206	0.05160	0.1	0.300039	0.1	0.042170	0.031	0.600	268	1	266.43	0.18	266.27	0.08
z8	0.646	1.8276	0.999	241	0.20	13956	0.205	0.05158	0.0	0.299868	0.1	0.042166	0.028	0.763	267	1	266.30	0.13	266.25	0.07
z6	**0.620**	**2.0705**	**0.998**	**160**	**0.33**	**9305**	**0.196**	**0.05158**	**0.1**	**0.299678**	**0.1**	**0.042136**	**0.028**	**0.699**	**267**	**1**	**266.15**	**0.17**	**266.06**	**0.07**
z5	**0.701**	**1.4384**	**0.998**	**185**	**0.20**	**10580**	**0.222**	**0.05158**	**0.1**	**0.299614**	**0.1**	**0.042127**	**0.032**	**0.700**	**267**	**1**	**266.10**	**0.16**	**266.00**	**0.08**
z4	**1.717**	**0.8942**	**0.998**	**165**	**0.18**	**7511**	**0.544**	**0.05157**	**0.1**	**0.299564**	**0.1**	**0.042127**	**0.033**	**0.621**	**267**	**2**	**266.06**	**0.20**	**266.00**	**0.09**
z1	**0.849**	**2.7419**	**0.999**	**278**	**0.27**	**15290**	**0.269**	**0.05154**	**0.1**	**0.299301**	**0.1**	**0.042120**	**0.033**	**0.434**	**265**	**2**	**265.85**	**0.20**	**265.96**	**0.09**
z9	**0.631**	**1.5792**	**0.998**	**172**	**0.24**	**9975**	**0.200**	**0.05160**	**0.0**	**0.299669**	**0.1**	**0.042120**	**0.032**	**0.758**	**268**	**1**	**266.14**	**0.16**	**265.96**	**0.08**
weighted mean ^{206}Pb/^{238}U age = 266.00 ± 0.04 (0.14) [0.31] Ma (2s); MSWD = 1.06 (n=5)																				
10VD-96																				
z4	0.443	2.2507	0.999	277	0.20	16893	0.140	0.05160	0.1	0.301623	0.1	0.042393	0.035	0.650	268	1	267.67	0.17	267.65	0.09
z6	0.434	2.8250	0.999	308	0.22	18843	0.137	0.05167	0.0	0.301935	0.0	0.042384	0.028	0.963	271	0	267.91	0.11	267.59	0.07
z10	**0.516**	**1.6215**	**0.998**	**194**	**0.21**	**11586**	**0.164**	**0.05165**	**0.0**	**0.301777**	**0.1**	**0.042375**	**0.028**	**0.757**	**270**	**1**	**267.79**	**0.14**	**267.54**	**0.07**
z3	**0.383**	**3.1905**	**0.999**	**289**	**0.27**	**17917**	**0.121**	**0.05168**	**0.0**	**0.301871**	**0.0**	**0.042363**	**0.030**	**0.937**	**271**	**1**	**267.86**	**0.12**	**267.46**	**0.08**
z5	**0.453**	**2.5301**	**0.999**	**313**	**0.20**	**19058**	**0.143**	**0.05162**	**0.0**	**0.301495**	**0.1**	**0.042361**	**0.032**	**0.746**	**269**	**1**	**267.57**	**0.14**	**267.45**	**0.09**
z8	**0.556**	**3.4060**	**0.992**	**39**	**2.23**	**2340**	**0.176**	**0.05160**	**0.1**	**0.301371**	**0.1**	**0.042358**	**0.035**	**0.591**	**268**	**2**	**267.47**	**0.22**	**267.43**	**0.09**
z7	**0.475**	**1.4587**	**0.998**	**190**	**0.19**	**11488**	**0.151**	**0.05161**	**0.1**	**0.301384**	**0.1**	**0.042351**	**0.030**	**0.633**	**268**	**1**	**267.48**	**0.17**	**267.39**	**0.08**
z1	0.506	8.4201	1.000	566	0.37	33925	0.160	0.05172	0.0	0.301565	0.0	0.042290	0.031	0.904	273	1	267.62	0.11	267.01	0.08
weighted mean ^{206}Pb/^{238}U age = 267.46 ± 0.04 (0.14) [0.31] Ma (2s); MSWD = 1.90 (n=5)																				

Notes:

(a) z1, z2 etc. are labels for single zircon crystals or fragments thereof, annealed and chemically abraded after Mattinson (2005).

(b) Model Th/U ratio calculated from radiogenic ^{208}Pb/^{206}Pb ratio and ^{207}Pb/^{235}U date.

(c) Pb* and Pbc are radiogenic and common Pb, respectively; mol % ^{206}Pb* is with respect to radiogenic and blank Pb.

(d) Measured ratio corrected for spike and fractionation only. Most samples are spiked with the ET2535 tracer, with internal Pb and U fractionation correction using the measured ^{202}Pb/^{205}Pb and ^{233}U/^{235}U.

(e) Corrected for fractionation, spike, common Pb, and initial disequilibrium in ^{230}Th/^{238}U. Up to 0.3 pg of common Pb is assigned to procedural blank with composition of ^{206}Pb/^{204}Pb = 18.042 ± 0.61%; ^{207}Pb/^{204}Pb = 15.537 ± 0.52%; ^{208}Pb/^{204}Pb = 37.686 ± 0.63% (1-sigma). Excess over blank was assigned to initial common Pb, using the Stacey and Kramers (1975) two-stage Pb isotope evolution model at 266 Ma.

(f) Errors are 2-sigma, propagated using algorithms of Schmitz and Schoene (2007).

(g) Calculations based on the decay constants of Jaffey et al. (1971). ^{206}Pb/^{238}U and ^{207}Pb/^{206}Pb ratios and dates corrected for initial disequilibrium in ^{230}Th/^{238}U using Th/U [magma] = 3.